2

Seasonal plasticity of mammalian diel activity rhythms: patterns and control

2.1 Abstract

The world is seasonal with animals subjected to predictable and periodic variations of the environment. Keeping track of these oscillations is relevant for reproduction and survival, and animals have evolved genetically programmed timing mechanisms, also called endogenous biological clocks, enabling circadian (24-hour) and circannual (365 days) rhythms to align with geophysical cycles; they use these to develop phenologies and to adapt to the time structure of the environment. Being essential to life but also energetically costly, activity level (movement) must be optimised throughout the day, and endogenous schedules are adjusted by environmental (exogenous) conditions. Among the numerous factors that influence the 24-hour circadian rhythm of a species, photoperiodism – which takes account of the measure of daylength and of the direction of change in daylength – is the most reliable environmental cue providing temporal information to synchronise circannual rhythms. In this study, camera trap systems were used to record patterns of seasonal occurrence within circadian rhythms of the mammal species of the Little Karoo in South Africa. The seasonal plasticity of the diel activity rhythm – defined in three time metrics: traditional 24-hour human clock-time and two ecological times with standardised sunrise and sunset times – is then quantified and compared among the species in the community. Most mammal species responded to the ecological variability brought about by seasonality

by adjusting their diel activity rhythms between winter and summer. Comparison of intraspecific shifts in diel activity rhythms – before and after time standardization in respect to annual sunrise and sunset times – showed that, while some shifts only result from photoperiodism alignment, most are driven by other factors too. Ten species shifted, in summer compared to winter, proportions of their daily activity from warmer daily time periods to cooler ones; this supports a behavioural strategy leading to a reduction of time exposure to a physiologically stressful environment caused by high temperatures in summer.

2.2 Introduction

The world is seasonal and, in most places, animals are subject to predictable and periodic variations of the environment; keeping track of these oscillations is relevant for reproduction and survival [109]. Resource availability or suitability often varies through the annual cycle, and is likely to influence species with lifespans of the order of a year or more [79, 200, 281, 299, 371]. Animals have evolved genetically programmed timing mechanisms, also called endogenous biological clocks, enabling circadian (24-hour) and circannual (365 days) rhythms, to align with geophysical cycles; they use these to develop phenologies and to adapt to the time structure of the environment [122, 139, 345]. Several species have been shown to have a persistent circannual cycles, sometimes throughout their lives, in the complete absence of temporal information, highlighting the underlying endogenous control [5,52,131,194,232]. However, under natural conditions, these rhythms vary between sympatric species as well as within species, depending on geographical location [12,236,258]. This suggests that these endogenous schedules can be adjusted by environmental (exogenous) conditions [73, 160, 370].

The diel activity rhythms of terrestrial mammals usually coincide with the hours of daylight, darkness, and/or twilight [19, 26, 151], and therefore they are usually grouped into four categories: diurnal, nocturnal, crepuscular (active in twilight) and cathemeral (irregularly active at any time of night or day) [8, 151]. Strictly nocturnal and strictly diurnal are two extremes of a continuum of temporal partitioning strategies over the 24-hour cycle [151]. Numerous factors influence the 24-hour circadian rhythm of a species [121, 190, 191, 275]. Ultimate factors provide the selective basis for biological seasonality, such as annual food and water availability, temperature [26] and interspecies interactions (predation and competition). Other factors (proximate factors), such as daylength [26, 74], are not themselves of

major importance to mammalian reproductive fitness but are employed to help time an organism's seasonal cycles and to anticipate and adapt to important changes in ultimate factors [122]. The most reliable environmental cue providing temporal information to synchronise circannual rhythms is the photoperiod, which takes account of the measure of daylength and of the direction of change in daylength [26, 38, 39, 109, 122, 244]. An encoded melatonin signal, secreted in concentrations inversely proportional to daylength, allows organisms to track time-of-year [122, 345].

Being essential to life but also energetically costly, activity level (movement) must be optimised throughout the day [82]. Defining the influence of seasonality on the diel activity of terrestrial mammals requires a large amount of data, collected among numerous individuals within the species community throughout the whole spectrum of the 24-hour and 365-day cycles. Animal activity level was traditionally measured through direct observations [25], or from data collected by telemetry devices [42, 165], such as speed of movement [257] and variance in signal strength [327]. More recently, multi-axial accelerometers have been used to collect high-resolution data on activity level [243]. Camera traps combine many advantages of the observational and telemetry-based techniques, while offering a number of improvements. Automation, miniaturization and networked systems are all features of modern camera traps, which enable ethologists to sample a variety of individuals and species within a community under greatly different environmental conditions. The disturbance caused by camera traps, despite some sounds and flashes [221], is likely to be minimal [3, 41, 128]. Time-of-detection data from remote sensors has been used to make inferences about animal activity level for many years [42, 59, 260, 290], and newly-developed analytical tools provide robust methods to quantify many aspects of animal behaviour from camera trap data [254, 283].

In this study, camera trap systems were used to record patterns of seasonal occurrence within circadian rhythms of the mammal species of the Little Karoo in South Africa. I then quantify and compare, for 25 frequently recorded mammal species, the seasonal plasticity of the diel activity rhythm defined in three time metrics: the traditional 24-hour human clock-time and two ecological times, in which the time of sunrise and sunset are transformed to be standardised throughout the 365-day cycle. The chapter finally shows whether seasonal shifts in animal diel activity rhythms are due to photoperiodism and/or to other factors.

2.3 Material and methods

2.3.1 Study area

The Little Karoo is a semi-arid desert located at the southern tip of the African continent [Appendix 1A], within the Cape Fold Belt [Introduction, Chapter 1 section 1.3.1]. Seasonality here involves the familiar temperate sequence of summer, autumn, winter and spring, but is largely driven by the cycle of a hot-dry summer, and a cool-wet winter [188]. Due to the inclination angle of the rotation axis of the Earth (as compared to its orbital plane), daylength varies with seasons on the planet's surface, depending on the observer's latitude. The study area in the Little Karoo is positioned in a grid cell with latitude-longitude coordinates for the north-west and south-east corners being respectively (33.296745°S ; 19.974518°E) and (33.916654°S ; 20.990753°E). The variation range of daylength in this area, between the southern summer solstice (14.40 hours on 21 December) and the southern winter solstice (9.92 hours on 22 June) is 4.48 hours.

2.3.2 Data collection

Camera traps were deployed between March 2014 and August 2015 [Chapter 1 section 1.3.2] as part of a research project on large carnivores – brown hyenas *Hyaena brunnea* and leopards *Panthera pardus* – within a study area of 4,327 km^2 (minimum convex polygon).

2.3.3 Analysis

2.3.3.1 Kernel density estimation

This analysis was designed to explore the seasonal plasticity of the diel activity of terrestrial mammals in the Little Karoo between winter (period of the year with daylength varying within the shortest third of its annual range), and summer (daylength varying within the longest third) (Fig. 2.1). The rest of the year, in which daylength varies within the middle third of its range, consists of two transitional time intervals; data collected for this period were discarded for this study.

The clock-times t recorded for every photo-capture i provided information on the diel activity rhythms of species s in winter and in summer. Season-specific diel activity rhythms were displayed using a 24-hour kernel density function k (flexible circular distribution [309]), which produced

the probability density function $A_{l,s}$ of the diel activity rhythm of species s throughout season l:

$$A_{l,s} = \sum_{i=1}^{n} k(t_{l_i,s}) \quad \text{with} \quad \int_0^{24} A_{l,s} \cdot dt = 1 \tag{2.1}$$
$$\text{In winter,} \quad l = w$$
$$\text{In summer,} \quad l = e \text{ (estival)}$$

The probability density functions $A_{l,s}$ are representations of circular distributions. Circular variables such as time-of-day are substantially different from linear variables because they do not behave like numbers on a number line (the 'distance' between 23:59 and 00:01 is the same as that between 10:41 and 10:43). The graphical display of circular distributions can therefore look very different depending on the selected time origin. For example, the diel activity rhythm of a strictly nocturnal species appears either as a unimodal or a U-shaped distribution, depending whether the display is centred around midnight or around noon (Fig. 2.4(a)). The graphical display of the probability density functions $A_{l,s}$ was either noon- or midnight-centred, depending on the time period of the 24-hour cycle in which most of the species' daily activity was allocated.

Every photo-capture was either defined as a capture-event or as a duplicate [Chapter 1 section 1.3.3]. All duplicates were discarded for this study because they inflate the photo-capture counts per unit of time and therefore distort the kernel density functions.

For this study, mammal species for which at least 15 photo-captures were made both in winter and in summer were included [Chapter 1 section 1.3.3]. The data collected within the northern section of the Sanbona Wildlife Reserve were discarded for this study due to the high game fence delimitating its border, which makes the reserve a biological system suspected to have evolved fairly independently and to differ from the rest of the study area [Chapter 1 section 1.3.1].

2.3.3.2 Data pre-processing

The diel activity rhythms of the mammals of the Little Karoo were analysed using three time metrics:

clock-time
In a first analysis, the unit of time t was the second (International System

of Units), defined in terms of oscillations of the caesium atom $_{55}$Cs [220]. It is the common unit for timekeeping used in human societies and it can unambiguously be defined as 'what a clock reads'.

Annual daylength standardisation

In human clock-time, sunrise and sunset times vary through the year and across study areas. Because the dark-light cycle is one of the most predictable environmental cue to which animals are subjected to, light entrainment is likely to be a significant driver of the endogenous circadian clock and associated diel activity rhythm [277]; analyses based on clock-time therefore result in 'fuzziness' of the activity timing, likely to particularly impact crepuscular species. In a second analysis, the time variable t was transformed so that daily sunrise and sunset times (SR, SS) were standardised to 06:38 (annual average of sunrise times $\overline{SR}$) and to 18:38 (annual average of sunset times $\overline{SS}$). However, the transformation did not affect true midday $\overline{MD}$ or midnight $\overline{MN}$, which were reached at 12:38 and 00:38 respectively, given the location of the study area on the Earth's surface.

$$\overline{SR} = 06{:}38 \ \ (6.63\ \text{h}) \qquad \overline{MD} = 12{:}38 \ \ (12.63\ \text{h})$$
$$\overline{SS} = 18{:}38 \ \ (18.63\ \text{h}) \qquad \overline{MN} = 00{:}38 \ \ (0.63\ \text{h})$$

This adjustment was achieved by pre-processing clock-time in both summer and winter datasets, by a pre-processing function f which varies with time of day t and date of year T:

$$t^{'} = f(t, T)$$

Although both winter and summer datasets were pre-processed according to the same set of rules, the variations of daylength between the two seasons resulted in two opposite time adjustments: time in summer was contracted around $\overline{SS}$ and $\overline{SR}$, whereas it was expanded in winter. However, $\overline{MD}$ and $\overline{MN}$ remained untransformed throughout the year and the magnitude of the time adjustment gradually decreased as t got closer to those two constant hours (Fig. 2.3 and Fig. 2.5).

The resulting $t^{'}$ was a 24-hour circular variable such that daylength equaled 12 hours, for all dates of winter and summer.

$$\text{With } t^{'} : \ \forall\, T, \ \text{daylength} = \overline{SS} - \overline{SR} = 12\ \text{h}$$

The sequential order of 'time distances' (or elapsed time) between different photo-capture events also remained the same before and after data preprocessing.

$$\forall\, (t_1, t_2) \in [0, 24], \ |t_1 - SR| \leq |t_2 - SR| \Leftrightarrow |t_1^{'} - \overline{SR}| \leq |t_2^{'} - \overline{SR}|$$

The pre-processing function f was defined by a set of four equations, applied to domains of t values, related to intervals between midnight and sunrise, sunrise and midday, midday and sunset, and sunset and midnight. SR and SS were respectively the sunrise and sunset times on the date T of the photo-capture, and t the time of the photo-capture event.

$$\begin{array}{lll} \overline{MN} \leq t \leq SR & t^{'} = \overline{MN} + K_1 \cdot (t - \overline{MN}) & K_1 = \dfrac{6}{SR - \overline{\overline{MN}}} \\ SR \leq t \leq \overline{MD} & t^{'} = \overline{MD} - K_2 \cdot (\overline{MD} - t) & K_2 = \dfrac{6}{\overline{\overline{MD}} - SR} \\ \overline{MD} \leq t \leq SS & t^{'} = \overline{MD} + K_3 \cdot (t - \overline{MD}) & K_3 = \dfrac{6}{SS - \overline{\overline{MD}}} \\ SS \leq t \leq \overline{MN} & t^{'} = \overline{MN} - K_4 \cdot (\overline{MN} - t) & K_4 = \dfrac{6}{\overline{\overline{MN}} - SS} \end{array} \tag{2.2}$$

Replacing $\overline{MD}$ and $\overline{MN}$ by their quantitative values for the study site yields:

$$\begin{array}{lll} 0.63 \leq t \leq SR & t^{'} = 0.63 + K_1 \cdot (t - 0.63) & K_1 = \dfrac{6}{SR - 0.63} \\ SR \leq t \leq 12.63 & t^{'} = 12.63 - K_2 \cdot (12.63 - t) & K_2 = \dfrac{6}{12.63 - SR} \\ 12.63 \leq t \leq SS & t^{'} = 12.63 + K_3 \cdot (t - 12.63) & K_3 = \dfrac{6}{SS - 12.63} \\ SS \leq t \leq 0.63 & t^{'} = 0.63 - K_4 \cdot (0.63 - t) & K_4 = \dfrac{6}{0.63 - SS} \end{array} \tag{2.3}$$

Time-of-day is a circular variable; under certain circumstances, the equations returned inappropriate time values for $t^{'}$. For example, if a species got photo-captured on 3 March at 23:00, four hours after sunset, then:

$$\left.\begin{array}{ll} t & = 23.00 \\ SS & = 19.00 \end{array}\right\} \; t^{'} = -6.67$$

To overcome this issue, the daily periodicity was defined as the 24-hour cycle starting at 00:38 (0.63) and finishing at 24:38 (24.63). Consequently, the fourth equation was then split up into two;

$$\begin{array}{lll} SS \leq t \leq 24 & t^{'} = 24.63 - K_{4.1} \cdot (24.63 - t) & K_{4.1} = \dfrac{6}{24.63 - SS} \\ 24 \leq t \leq 24.63 & t^{'} = 24.63 - K_{4.2} \cdot (24.63 - t) & K_{4.2} = \dfrac{6}{24.63 - SS_p} \end{array} \tag{2.4}$$

where SS_p is the sunset time on the previous day $(T - 1)$ of the photo-capture.

In the five equations (Eq. 2.3 and 2.4), the distortion of t was mainly defined by the value of the coefficient K_λ which, depending on the season, was either greater or smaller than 1. Fig. 2.3 shows the pre-processing of t for events that took place on the days of the winter and summer solstices. It highlights

the standardisation of daylength to exactly 12 hours throughout the 365-day cycle. Fig. 2.5 provides a different approach to showing the results of the pre-processing function f for all values of t within the 24-hour cycle, but this time for events that took place on six dates of the year T, including on the vernal and fall equinoxes T_4 as well as on the southern summer and winter solstices (T_1, T_6). Photo-capture events that took place during winter mornings saw their times t adjusted to earlier values (blue points below the black line $y = x$), whereas events that took place during winter afternoons, saw their times t adjusted to later values (blue points above the black line), resulting in an expansion of daylength (grey area in Fig. 2.5). The opposite transformation took place in summer with a contraction of daylength (white area in Fig. 2.5).

$$\left.\begin{array}{ll} \text{winter} & \overline{MN} < t < \overline{MD} \Rightarrow \ t^{'} < t \\ \text{winter} & \overline{MD} < t < \overline{MN} \Rightarrow \ t^{'} > t \end{array}\right\} \text{daylength expansion}$$

$$\left.\begin{array}{ll} \text{summer} & \overline{MN} < t < \overline{MD} \Rightarrow \ t^{'} > t \\ \text{summer} & \overline{MD} < t < \overline{MN} \Rightarrow \ t^{'} < t \end{array}\right\} \text{daylength contraction}$$

$t^{'}$ values greater than 24.00 ($24 \leq t \leq 24.63$) were then re-adjusted by subtracting 24.00, so that all $t^{'}$ values belonged to the 24-hour cycle starting at 00:00 and finishing at 24:00.

Using $t^{'}$ as circular data, the probability density functions describing the diel activity rhythms $A_{l,s}$ of species s during season l, in relation to sunrise and sunset, were computed.

Seasonal daylength standardisation

Finally, in a third analysis, the time variable t was also transformed so that summer and winter activity patterns could be compared, by standardising daily sunrise times SR to 07:25 (winter average of sunrise times $\overline{SR}_w$) or to 05:40 (summer average of sunrise times $\overline{SR}_e$), and daily sunset times SS to 17:53 (winter average of sunset times $\overline{SS}_w$) or to 19:31 (summer average of sunset times $\overline{SS}_e$). However, the transformation did not affect true midday $\overline{MD}$ and night $\overline{MN}$, which were reached at 12:38 and 00:38 respectively, given the location of the study area on the Earth's surface.

$$\begin{array}{lll} \overline{SR}_e = 05{:}40 \ (5.67\,\text{h}) & \overline{SR}_w = 07{:}25 \ (7.42\,\text{h}) & \overline{MD} = 12{:}38 \ (12.63\,\text{h}) \\ \overline{SS}_e = 19{:}31 \ (19.52\,\text{h}) & \overline{SS}_w = 17{:}53 \ (17.88\,\text{h}) & \overline{MN} = 00{:}38 \ (0.63\,\text{h}) \end{array}$$

This adjustment was achieved by pre-processing clock-time according to a similar method, except that in this case, two different and seasonal pre-

processing functions f_l were applied to winter (f_w) and summer (f_e) datasets:

$$f_l(t,T)\begin{cases} T \in \text{winter}, & t' = f_e(t,T) \\ T \in \text{summer}, & t' = f_w(t,T) \end{cases}$$

Winter and summer datasets were pre-processed according to different sets of rules: time in summer was slightly contracted around $\overline{SR}_e$ and $\overline{SS}_e$, whereas it was slightly expanded in winter around $\overline{SR}_w$ and $\overline{SS}_w$.

The resulting t'' was a 24-hour circular variable, and the difference of daylength between any winter and summer days was always equal to exactly 3.37 hours.

$$(\overline{SS}_e - \overline{SR}_e) - (\overline{SS}_w - \overline{SR}_w) = 3.37 \text{ h}$$

The sequential order of 'time distance' between different photo-capture events remained the same before and after data pre-processing.

$$\forall\, l \in \{w,e\},\ \forall\, (t_1,t_2) \in [0,24],$$
$$|t_1 - SR_l| \leq |t_2 - SR_l| \Leftrightarrow |t_1' - \overline{SR}_l| \leq |t_2' - \overline{SR}_l|$$

The pre-processing function f_l of season l only differed from its sister function f by the numerator n_λ of the K_λ coefficients in all five equations (Eq. 2.3 and 2.4). $\lambda \in \{1,2,3,4,5\}$:

$$\begin{array}{lll} 0.63 \leq t \leq SR & n_{1,w} = 6.79 & n_{1,e} = 5.06 \\ SR \leq t \leq 12.63 & n_{2,w} = 5.21 & n_{2,e} = 6.94 \\ 12.63 \leq t \leq SS & n_{3,w} = 5.25 & n_{3,e} = 6.89 \\ SS \leq t \leq 24.00 & n_{4,w} = 6.74 & n_{4,e} = 5.10 \\ 24.00 \leq t \leq 24.63 & n_{5,w} = 6.74 & n_{5,e} = 5.10 \end{array} \quad (2.5)$$

t'' values greater than 24.00 ($24 \leq t \leq 24.63$) were then re-adjusted by subtracting 24.00, so that all t'' values belonged to the 24-hour cycle starting at 00:00 and finishing at 24:00.

Using t'' as circular data, the probability density functions describing the diel activity rhythms $A''_{l,s}$ of species s during season l, in relation to seasonal times of sunrise and sunset, were computed.

2.3.3.3 Bootstrapping

A statistical bootstrap method (resampling technique) [235] was used to compare, for every mammal species s, its diel activity rhythm from the data collected during winter $A_{w,s}$ to that collected during summer $A_{e,s}$.

Kernel density functions such as $A_{l,s}$ have an under-curve area equal to 1, which offers the opportunity to compare them against one another, by calculating their coefficient of overlap ranging from 0 (no overlap) to 1 (identical curves) [283]. Using the *overlapEst* function from the *overlap* R-package [226], the coefficient of overlap $O_{,s}$ in diel activity rhythms of species s, between winter and summer was calculated:

$$\begin{aligned} O_{,s} &= O_v(A_{w,s},\ A_{e,s}) \\ &= \int_0^{24} \min(A_{w,s},\ A_{e,s}) \cdot dt \end{aligned} \tag{2.6}$$

The process of bootstrapping consists of random sampling without replacement (also called permutation). In this study, $r = 10,000$ permutations were created by randomly splitting the camera trap dataset into two samples ($A_{w_p,s}$, $A_{e_p,s}$) with sizes matching those of the two datasets obtained during the winter and summer seasons. Similarly, the coefficient of overlap of the two newly created density functions was calculated, prior to storing it into a species vector $V_{,s}$:

$$\begin{gathered} O^p_{,s} = O_v(A_{w_p,s},\ A_{e_p,s}) \\ V_{,s} = (O^1_{,s},\ O^2_{,s},\ \ldots\ O^p_{,s},\ \ldots\ O^r_{,s}) \\ r = 10,000 \end{gathered} \tag{2.7}$$

The percentage of overlap coefficients stored in $V_{,s}$ that are greater than the observed one $O_{,s}$ was calculated for every species s, along with the p-value $P_{,s}$:

$$\begin{gathered} V_{g,s} = \text{subset}(V_{,s},\ O^p_{,s} > O_{,s}) \\ P_{,s} = \frac{L(V_{g,s})}{L(V_{,s})} \qquad L = \text{length}() \end{gathered} \tag{2.8}$$

The bootstrap analysis was applied to the three pre-processed datasets, built with three different time variables t, $t^{'}$ and $t^{''}$, producing $O_{,s}$, $O^{'}_{,s}$, $O^{''}_{,s}$ and $P_{,s}$, $P^{'}_{,s}$, $P^{''}_{,s}$.

2.3.3.4 Circular statistics

The statistical analysis of circular data is a specialised field [108, 156]. Batschelet (1981) [21] deals with circular statistics specifically within a biological framework. When standard statistical measures, such as the arithmetic mean and variance are applied to circular variables, inappropriate

and nonsensical results are obtained, depending on the arbitrary time origin [21]. Batschelet (1981) [21] provides mathematical tools (vector algebra and trigonometric functions) to measure location and dispersion within a circular distribution. These mathematical tools offer an opportunity to profile species' diel activity rhythms and to quantify their seasonal shifts. However, this methodology provides meaningful results under the assumption that data are symmetric and unimodal, and very few mammal species of the Little Karoo have their diel activity rhythms meet those criteria (Fig. 2.4(b)), which is why other routes had to be explored.

2.3.3.5 Seasonal shift in diel activity rhythms

The seasonal shift in diel activity rhythms between summer and winter was quantified in the three different time metrics t, $t^{'}$ and $t^{''}$, for the 25 mammal species s:

$$\begin{aligned} S_{,s} &= A_{e,s} - A_{w,s} \\ S^{'}_{,s} &= A^{'}_{e,s} - A^{'}_{w,s} \\ S^{''}_{,s} &= A^{''}_{e,s} - A^{''}_{w,s} \end{aligned} \tag{2.9}$$

$S_{,s}$, $S^{'}_{,s}$ and $S^{''}_{,s}$ could also be defined as:

$$\int_0^{24} S_{,s} \cdot dt = \int_0^{24} S^{'}_{,s} \cdot dt^{'} = \int_0^{24} S^{''}_{,s} \cdot dt^{''} = 0 \tag{2.10}$$

$$\int_0^{24} |S_{,s}| \cdot dt = 2 \cdot (1 - O_{,s})$$

$$\int_0^{24} |S^{'}_{,s}| \cdot dt^{'} = 2 \cdot (1 - O^{'}_{,s}) \tag{2.11}$$

$$\int_0^{24} |S^{''}_{,s}| \cdot dt^{''} = 2 \cdot (1 - O^{''}_{,s})$$

The area under the curve of probability density functions is, by definition, equal to 1; the definite integrals of the difference between two such functions is compulsorily equal to 0 (Eq. 2.10). The demonstration of Eq. 2.11 is provided in Appendix 4A.

Descriptive statistics

In Chapter 3 section 3.4, it was shown that, after daylength standardisation

($t^{'}$) and within the 24-hour cycle, the time-profile (summary of the activity level of all species in the community at time $t^{'}$) went through a periodic cycle characterised by four periods θ. Two stable ones ϕ_n and ϕ_d, matching the darkest and brightest hours of the cycle. Outside those hours, the time-profile went through two transitional periods ρ_m and ρ_e during which it varies rapidly to get from ϕ_n to ϕ_d and vice versa. The early morning and late evening periods (ρ) are therefore considered to be the crepuscular hours of the daily cycle.

$$\theta \begin{cases} \phi_n & : \quad (\overline{SS} + 1.37 \text{ h}, \ \overline{SR} - 1.63 \text{ h}) \\ \phi_d & : \quad (\overline{SR} + 3.37 \text{ h}, \ \overline{SS} - 2.63 \text{ h}) \\ \rho_m & : \quad (\overline{SR} - 1.63 \text{ h}, \ \overline{SR} + 3.37 \text{ h}) \\ \rho_e & : \quad (\overline{SS} - 2.63 \text{ h}, \ \overline{SS} + 1.37 \text{ h}) \end{cases} \tag{2.12}$$

ρ_m, ϕ_d, ρ_e and ϕ_n respectively last five, six, four and nine hours.

Several descriptive statistics were then defined and calculated for every species s and for the four daily time periods θ defined above. These statistics were annotated with an apostrophe to highlight the fact that there were calculated after annual daylength standardisation of the data ($t^{'}$):

$$\begin{aligned} &\text{Total rhythm variation (\%):} && \text{TRV}^{'}_{,s} = \frac{1}{2} \cdot 100 \cdot \int_0^{24} |S^{'}_{,s}| \cdot dt^{'} \\ &\text{Local rhythm variation (\%):} && \text{LRV}^{'}_{,s}(\theta) = 100 \cdot \frac{\int_\theta |S^{'}_{,s}| \cdot dt^{'}}{\int_0^{24} |S^{'}_{,s}| \cdot dt^{'}} \\ &\text{Local activity shift (\%):} && \text{LAS}^{'}_{,s}(\theta) = 100 \cdot \int_\theta S^{'}_{,s} \cdot dt^{'} \\ &\text{Compensation index:} && I^{'}_{,s}(\theta) = \frac{\int_\theta S^{'}_{,s} \cdot dt^{'}}{\int_\theta |S^{'}_{,s}| \cdot dt^{'}} \end{aligned} \tag{2.13}$$

The mathematical relationships between $A^{'}_{l,s}$, $O^{'}_{,s}$ and $S^{'}_{,s}$ are defined in Fig. 2.6.

The total rhythm variation of species s ($\text{TRV}^{'}_{,s}$) provides the percentage of diel activity rhythm that shifted between the two seasons. The local rhythm variation of species s during time period θ ($\text{LRV}^{'}_{,s}(\theta)$) provides the percentage of $\text{TRV}^{'}_{,s}$ explained during θ. The local activity shift of species s during time period θ ($\text{LAS}^{'}_{,s}(\theta)$) provides the resulting shift in daily activity proportions allocated by species s throughout θ. Finally, the compensation index of species s during time period θ ($I^{'}_{,s}(\theta)$) will be equal to 1 if $\text{LRV}^{'}_{,s}(\theta)$ is entirely converted into a shift in activity. However, if compensation effects (activity

increases compensated by activity decreases throughout θ) occur, $I^{'}_{,s}(\theta)$ will take values greater than one.

After this species-specific work, the same analysis was applied to the whole mammal community c, using the following probability density functions:

$$\int_0^{24} A_{l,c} \cdot dt = \int_0^{24} A^{'}_{l,c} \cdot dt^{'} = \int_0^{24} A^{''}_{l,c} \cdot dt^{''} = 1 \tag{2.14}$$

$A_{l,c}$, $A^{'}_{l,c}$ and $A^{''}_{l,c}$ were calculated using the data for the 25 mammal species within the community c. The following variables $S_{,c}$, $S_{,c}{}^{'}$ and $S_{,c}{}^{''}$, as well as descriptive statistics $\text{TRV}^{'}_{,c}$, $\text{LRV}^{'}_{,c}$, $\text{LAS}^{'}_{,c}$ and $I^{'}_{,c}$, were calculated. The weight a species s had on the diel activity rhythms of the mammal community c, was proportional to its photo-capture frequency.

At a second stage, diel activity rhythms $A_{l,\bar{c}}$, $A^{'}_{l,\bar{c}}$ and $A^{''}_{l,\bar{c}}$ were built using equal weight for the 25 mammal species within the community $\bar{c}$. This was achieved by extracting, for every species s, 128 points at regular time intervals from each of the three kernel density functions $A_{l,s}$, $A^{'}_{l,s}$ and $A^{''}_{l,s}$, before averaging:

$$\begin{aligned}
i \in [1..128], \qquad A_{l,\bar{c}}(t_{l_i}) &= \frac{\sum_{s_j=1}^{25} A_{l,s_j}(t_{l_i})}{25} \\
i \in [1..128], \qquad A^{'}_{l,\bar{c}}(t^{'}_{l_i}) &= \frac{\sum_{s_j=1}^{25} A^{'}_{l,s_j}(t^{'}_{l_i})}{25} \\
i \in [1..128], \qquad A^{''}_{l,\bar{c}}(t^{''}_{l_i}) &= \frac{\sum_{s_j=1}^{25} A^{''}_{l,s_j}(t^{''}_{l_i})}{25}
\end{aligned} \tag{2.15}$$

Applying the same analysis once more, following variables $S_{,\bar{c}}$, $S_{,\bar{c}}{}^{'}$ and $S_{,\bar{c}}{}^{''}$, as well as descriptive statistics $\text{TRV}^{'}_{,\bar{c}}$, $\text{LRV}^{'}_{,\bar{c}}$, $\text{LAS}^{'}_{,\bar{c}}$ and $I^{'}_{,\bar{c}}$, were calculated.

Non-metric Multi-Dimensional Scaling (NMDS)

Non-metric approach to multi-dimensional scaling is a statistical tool which provides a means of displaying and summarising a square symmetric matrix of dissimilarities into a low-dimensional Euclidean space [126, 180, 181]. A dissimilarity matrix was computed to estimate the dissimilarities of seasonal shifts in diel activity rhythm for each pair of species in the mammal

community of the Little Karoo [32]. The objective in NMDS is to find a configuration of points in Euclidean space so that the ordering of the interpoint distances matches, as closely as possible, the ordering of the dissimilarities in the matrix of dissimilarities [32].

The information contained in $S'_{,s}$ was compiled into a matrix M with $n = 25$ rows (species) and $p = 128$ columns (t' values selected at regular intervals between 00:38 and 24:38). Every element $M[s, t']$ gave the seasonal change in diel activity rhythm $S'_{,s}(t')$ of species s at time t'.

$$M[s,\ t'] = S'_{,s}(t')$$

Using the *dist* function from the *stats* R-package [22, 32, 209], M was computed to calculate a distance matrix with distances being measured between rows of M using the Manhattan method; the output distance matrix was a symmetric matrix with 25 rows and columns, and was referred to as the Activity-shift Distance Matrix (ADM). Every element ADM$[s_1,\ s_2]$ quantified the dissimilarity between the seasonal shift in diel activity rhythm of species s_1 and s_2.

$$\text{ADM}[s_1,\ s_2] = \text{dist}(S'_{,s_1},\ S'_{,s_2})$$

An NMDS ordination was performed on ADM, using the *isoMDS* function from the *MASS* R-package [285]. Summarising a dissimilarity matrix into a two-dimensional plot might not be feasible and a certain amount of distortion might be created. The measure of lack of fit in NMDS is known as the 'stress' of the configuration. Non-zero stress values occur with insufficient dimensionality, and as the number of dimensions increases, the stress value will either decrease or remain stable [32]. The objective of the ordination is to find the configuration with minimum 'stress' for a given number of dimensions. The operation was therefore repeated several times with a different number of chosen dimensions k, and a screeplot (stress versus k) was plotted in order to identify the point beyond which additional dimensions do not substantially lower the stress value.

2.4 Results

The trapping effort of 14,331 camera trap nights resulted in 21,469 photo-captures which were reduced to 9,057 independent photo-capture events; these involved 80 wild species, including 46 mammals, 33 birds and one reptile. Of the 46 mammal species, 25 had more than 15 photo-captures in both summer and winter to enable the analysis to be conducted [Appendix 2A].

2.4.1 Diel activity rhythms

The probability density functions, built with the three time metrics, described the noon- or midnight-centred diel activity rhythms $A_{l,s}$, $A'_{l,s}$ and $A''_{l,s}$ of species s during season l, and showed the nocturnal-diurnal dichotomy that provides a temporal axis of niche segregation and that has facilitated coexistence among sympatric species [40] [Chapter 3 section 3.4] (Fig. 2.7). Similarly, Fig. 2.9 displays the diel activity rhythms $A_{l,c}$, $A'_{l,c}$ and $A''_{l,c}$, as well as $A_{l,\bar{c}}$, $A'_{l,\bar{c}}$ and $A''_{l,\bar{c}}$ of the mammal community c and $\bar{c}$ during season l.

2.4.2 Overlap coefficients

The associated overlap coefficients calculated between seasonal diel activity rhythms were shaded in grey (Fig. 2.7 and 2.9), and summarised in Table 2.1.

The diel activity rhythms of the 25 mammal species s were nearly identical before and after **seasonal** daylength standardisation ($A_{l,s}$, $A''_{l,s}$). The average difference between their associated overlap coefficients $O_{,s}$ and $O''_{,s}$ was equal to 0.8% (Table 2.1).

The average difference in overlap $O_{,s}$ and $O'_{,s}$ between the diel activity rhythms of the 25 mammal species s, produced before and after **annual** daylength standardisation $A_{l,s}$ and $A'_{l,s}$, was however substantial and equal to 7.3%. The graphs in Fig. 2.7 illustrate the distortion t' of the linearity of clock-time t around sunrise and sunset (contraction in summer, expansion in winter), due to annual daylength standardisation. For 20 of the 25 mammal species, standardising daily times of sunrise and sunset (SR, SS) to the annual average times of sunrise and sunset ($\overline{SR}$, $\overline{SS}$) prompted an increase in overlap $O'_{,s}$, sometimes as high as 15% (e.g. leopard and grey duiker *Sylvicapra grimmia*). Aardvark *Orycteropus afer*, Cape hare *Lepus capensis*, red hartebeest *Alcelaphus buselaphus* and scrub hare *Lepus saxatilis* were the four species having their overlap coefficients decreasing after annual daylength standardisation, that of aardowlf *Proteles cristatus* remained constant. $O'_{,s}$ ranged from 0.46 (rock hyrax *Procavia capensis*, greatest seasonal change) to 0.89 (greater kudu *Tragelaphus strepsiceros*, smallest seasonal change).

2.4.3 Bootstrapped p-values

The results of the bootstrap analysis are summarised in Table 2.1 and Fig. 2.10. They showed that the significant seasonal shift in clock-timed diel

activity rhythms between winter and summer ($P_{,s} < 0.05$) for African wildcat *Felis silvestris*, Cape mountain zebra *Equus zebra zebra*, greater kudu and leopard, was no longer observed after annual daylength standardisation ($P'_{,s} > 0.05$). It however remained observed ($P_{,s} < 0.05$ and $P'_{,s} < 0.05$) for 15 other species: aardwolf, black-backed jackal *Canis mesomelas*, Cape gray mongoose *Galerella pulverulenta*, Cape porcupine *Hystrix africaeaustralis*, caracal *Caracal caracal*, chacma baboon *Papio ursinus*, eland *Taurotragus oryx*, gemsbok *Oryx gazella*, grey duiker, honey badger *Mellivora capensis*, Hewitt's red rock rabbit *Pronolagus saundersia*, klipspringer *Oreotragus oreotragus*, rock hyrax *Procavia capensis*, scrub hare *Lepus saxatilis* and steenbok *Raphicerus campestris*.

The bootstrap analysis also showed that three of the six species which displayed no significant seasonal change in their clock-timed diel activity rhythms between winter and summer ($P_{,s} > 0.05$), did display a significant change after annual daylength standardisation ($P'_{,s} < 0.05$): aardvark *Orycteropus afer*, Cape hare *Lepus capensis* and red hartebeest *Alcelaphus buselaphus*.

2.4.4 Seasonal shift in diel activity rhythm

Seasonal shift in diel activity rhythm were displayed using S-curves (Fig. 2.8 and 2.9), before being explored using descriptive statistics (Table 2.2).

2.4.4.1 Graphical display: S-curves

The summer-winter seasonal shifts in diel activity rhythms for each of the 25 mammal species s, were quantified for the three time metrics, and represented as noon- or midnight-centred curves $S_{,s}$, $S'_{,s}$ and $S''_{,s}$ in Fig. 2.8. Similarly, Fig. 2.9 displays the summer-winter seasonal shifts in diel activity rhythms $S_{,c}$, $S'_{,c}$ and $S''_{,c}$ as well as $S_{,\bar{c}}$, $S'_{,\bar{c}}$ and $S''_{,\bar{c}}$, of the mammal community c and $\bar{c}$. In each two-dimensional Euclidean space, the signed area of the plane that was bounded by the S'-curve, the horizontal line $y = 0$, and the vertical lines $t' = 0$ and $t' = 24$, was shaded in black over the darkest hours of the cycle (ϕ_n), dark grey over the crepuscular hours (ρ) and light grey over the brightest hours (ϕ_d). The species-specific seasonal shifts $S_{,s}$, $S'_{,s}$ and $S''_{,s}$ were positive when the proportion of daily activity, allocated by species s at time t, t' and t'', was higher in summer than in winter. On the contrary, they were negative when the proportion was lower in summer than in winter. The same observations applied to communal seasonal shifts $S_{,c}$, $S'_{,c}$ and $S''_{,c}$ as well as $S_{,\bar{c}}$, $S'_{,\bar{c}}$ and $S''_{,\bar{c}}$.

2.4.4.2 Descriptive statistics

Table 2.2 compiles the S-curves descriptive statistics TRV', LRV', LAS' and I' providing insights into the seasonal shifts in diel activity rhythms of the 25 mammal species s and of the whole mammal community c and $\bar{c}$.

a) Total rhythm variation: $\text{TRV}'_{,s}$

The 25 mammal species were ranked in descending order of their total rhythm variation $\text{TRV}'_{,s}$ (Table 2.2). Rock hyrax, with 54% of $\text{TRV}'_{,s}$, was the species with the highest percentage of diel activity rhythm shift between summer and winter. Greater kudu was the species with the lowest percentage of diel activity rhythm shift between summer and winter (11% of $\text{TRV}'_{,s}$). High percentages of $\text{TRV}'_{,s}$ did not necessarily imply a significant seasonal shift in diel activity rhythm. With 28% of $\text{TRV}'_{,s}$, Springbok showed a substantial variation of its seasonal diel activity rhythms; however, the bootstrap analysis showed no significant change (Table 2.1).

b) Local rhythm variation: $\text{LRV}'_{,s}(\theta)$

The percentage of $\text{TRV}'_{,s}$ explained during each of the four θ time periods (ρ_m, ϕ_d, ρ_e and ϕ_n (Eq. 2.12)), was defined as the associated local rhythm variation $\text{LRV}'_{,s}(\theta)$. Divided by the number of hours in θ, it provided the hourly rhythm variation of species s throughout θ (Table 2.2). $\text{LRV}'_{,s}(\theta)$ was shaded in grey when θ was the time period of the 24-hour cycle with the highest hourly rhythm variation. The variations in diel activity rhythm took place throughout the 24-hour cycle and the time period θ that explained most of those variations varied according to the species. For eight of the 25 species, the seasonal shift mainly took place throughout the crepuscular hours of the morning (ρ_m). Eight other species showed a main shift during the darkest hours (ϕ_n), five species during the crepuscular hours of the evening (ρ_e) and four species during the brightest hours (ϕ_d). When considering all crepuscular hours together (ρ), it appeared that, for 13 species, most of the seasonal shift took place during the crepuscular hours of the 24-hour cycle. This is also true regarding the variations in diel activity rhythm of the mammal community as a whole: c and $\bar{c}$.

c) Local activity shift: $\text{LAS}'_{,s}(\theta)$

Variations of the diel activity rhythm can lead to local activity shifts: increases and/or decreases in the proportions of daily activity allocated to certain time periods of the 24-hour cycle. They can also result in no alteration of the proportions of daily activity during a specific time period (θ), because of compensation effects (throughout the time period in question, local increases can be compensated by local decreases).

Morning crepuscular hours, $\text{LAS}'_{,s}(\rho_m)$: Table 2.2 shows that, except for honey badger and leopard, the other 23 mammal species increased their proportions of daily activity allocated to morning crepuscular hours (ρ_m) in summer, compared with those allocated in winter. These percentages were shaded in orange.

Brightest and evening crepuscular hours, $\text{LAS}'_{,s}(\phi_d, \rho_e)$: The proportions of daily activity allocated to brightest hours (ϕ_d) and evening crepuscular hours (ρ_e) in summer, decreased (shaded in blue) or remained unchanged (no shading) for most species (23 species for ϕ_d, and 20 species for ρ_e).

Darkest hours, $\text{LAS}'_{,s}(\phi_n)$: The trends regarding the darkest hours (ϕ_n) were more nuanced with roughly the same number of species having increased (8 species) their proportions of daily activity during the darkest hours of the 24-hour cycle in summer, as the number of species having decreased (10 species) or unchanged (seven species) their proportions of daily activity during those hours.

One of the most striking seasonal shift was that of honey badger. It displayed a bimodal and crepuscular pattern in winter and a unimodal and nocturnal pattern in summer (Fig. 2.7(r)).

d) Compensation index: $I'_{,s}(\theta)$

Four species, klipspringer, steenbok, Cape porcupine and African wildcat, showed substantial compensation effects, meaning that despite large seasonal variations of their diel activity rhythms over θ, their resulting seasonal shift in activity during θ was small. The compensation index $I'_{,s}(\theta)$ highlighted these compensation effects with values appreciably greater than one, and shaded in grey in Table 2.2. For 14 species, the compensation index $I'_{,s}(\rho)$ was greater than one, meaning that the seasonal shift in activity allocated to morning and evening crepuscular hours (ρ_m and ρ_e) worked in opposite directions. When a species showed no activity during θ in both seasons, the associated $\text{LRV}'_{,s}(\theta)$ and $\text{LAS}'_{,s}(\theta)$ were zero, and $I'_{,s}(\theta)$ returned NA.

Looking at the mammal community $\bar{c}$, the seasonal variations in diel activity rhythm led to an increase of the proportions of daily activity allocated to morning crepuscular hours (ρ_m), a decrease of the proportions of daily activity allocated to the brightest and evening crepuscular hours (ϕ_d and ρ_e), and no shift in proportions of daily activity allocated to the darkest hours of the night (ϕ_n). However, $I'_{,\bar{c}}(\phi_n) = 11$ showed that the proportions of daily activity symmetrically increased and decreased at different periods of the darkest time period (ϕ_n), creating activity compensation. Finally, $I'_{,\bar{c}}(\rho) = 4$ showed that the proportions of daily activity varied in opposite directions be-

tween morning and evening crepuscular hours (ρ_m and ρ_e). Fig. 2.9 provides a graphical summary of those results.

2.4.5 Seasonal shift comparison in the community

The NMDS algorithm captured, in two dimensions, the essential structure of the dissimilarity data (stress = 0.159). Fig. 2.11 represents, as closely as possible, the ordering of the dissimilarities between species' seasonal shift in diel activity rhythm. In other words, points close together represent species that shifted their diel activity rhythm between winter and summer in a more similar manner than species represented by points farther apart; however, the graph does not provide quantitative information regarding this difference. Whenever possible, the noon-centred $S'_{,s}$-curves were added to NMDS plot, next to the associated species points.

A screeplot (Fig. 2.12) revealed that attempting an ordination with one NMDS axis yielded unacceptably high stress (0.269) whereas two or three dimensions was more adequate. However, with five dimensions, the stress value dropped below 0.050, which indicated good fit. Despite a stress value greater than 0.050, the NMDS plot in two dimensions could be useful as a first exploration of the data and to gain some insights into the dissimilarities data between the seasonal shifts in diel activity rhythm of the 25 mammal species s, within the mammal community of the Little Karoo.

In the NMDS plot (Fig. 2.11), the 25 mammal species were spatially placed in a plane with a clear and gradual left-right transition along the first axis, from species with a 'diurnal' shift of their diel activity rhythms between summer and winter (e.g. rock hyrax) to species with a 'nocturnal' shift of their diel activity rhythms between summer and winter (e.g. aardwolf). The species in the centre of the plot are those which show rather little pattern and small-amplitude shifts of their diel activity rhythms between seasons (e.g. greater kudu). Species on the right hand side of the first axis are the species which are nocturnal, but switch from using hours before midnight in winter to hours after midnight in summer, of which aardwolf is the strongest example. On the edges of the plot are the species with unusual shifts: rock hyrax remains diurnal but switches a substantial proportion of its daily activity from midday hours in winter to morning twilight in summer; honey badger shifts from being crepuscular in winter to being nocturnal in summer; and red hartebeest, which is crepuscular both seasons, but switches a substantial proportion of its daily activity from night to day.

2.5 Discussion

Using camera traps set over winter and summer, this chapter documented the seasonal plasticity of the diel activity rhythms of 25 mammal species co-occurring in the Little Karoo. Most mammal species responded to the ecological variability brought about by adjusting their diel activity rhythms between winter and summer. The extent of these seasonal shifts varied among the mammal community.

2.5.1 Data pre-processing

Standardising daily times of sunrise and sunset (SR, SS) to the **annual** average times of sunrise and sunset ($\overline{SR}$, $\overline{SS}$), reshaped species' diel activity rhythms noticeably. In contrast, standardising daily times of sunrise and sunset (SR, SS) to the **seasonal** average times of sunrise and sunset ($\overline{SR}_w$, $\overline{SR}_e$; $\overline{SS}_w$, $\overline{SS}_e$), hardly influenced species' diel activity rhythms, because of the minor time difference between t and t''. On any day of season l, sunrise and sunset times were close to the seasonal averaged ones, which is why pre-processing the data in this manner brought no useful insights into the seasonal shifts in diel activity rhythms of the 25 sympatric mammal species.

2.5.2 Factors influencing seasonal shifts

The de-synchronised, clock-timed diel activity rhythms of African wildcat, Cape mountain zebra, greater kudu and leopard were synchronised with annual daylength standardisation, meaning that, for these species, the seasonal change in diel activity rhythms was almost entirely a consequence of photoperiodism alignment.

The de-synchronised, clock-timed diel activity rhythms of aardwolf, black-backed jackal, Cape gray mongoose, Cape porcupine, caracal, chacma baboon, eland, gemsbok, grey duiker, honey badger, Hewitt's red rock rabbit, klipspringer, rock hyrax, scrub hare and steenbok, did not re-synchronise after annual daylength standardisation, suggesting that their significant seasonal change in diel activity rhythms were not (solely) a result of photoperiodism alignment, and was driven by other factor(s). However, except for aardwolf and scrub hare, the overlap coefficients of the other 13 species increased after annual daylength standardisation ($O'_{,s} > O_{,s}$), often further to a minimisation of the seasonal de-synchronisation, which suggests that their significant seasonal change in diel activity rhythms could be a partial conse-

quence of photoperiodism alignment as well, whose contribution increased as their overlap coefficient did too.

The synchronised, clock-timed diel activity rhythms of aardvark, Cape hare and red hartebeest got de-synchronised, and their overlap coefficient decreased, after annual daylength standardisation, meaning that their diel activity rhythms did not align to photoperiodism as seasons change and that they follow clock-time.

Finally, no significant seasonal change in clock-timed and t'-adjusted diel activity rhythms was observed for brown hyena, grey rhebuck and springbok. The increase of their overlap coefficient after annual daylength standardisation suggests that their diel activity rhythms might partly align to photoperiodism. This adjustment would however not be significant given the overall versatility of the diel activity rhythm.

Comparing intraspecific shifts in diel activity rhythms – before and after time standardization in respect to annual sunrise and sunset times – this chapter found that, while some shifts only result from photoperiodism alignment, most are driven by other factors too (Table 2.3). Environmental seasonality influences processes that enable individuals to meet their metabolic needs; it drives population dynamics and community structure. It also translates into variations of numerous environmental factors such as phototoperiodism, temperature, rainfall and food availability [46]. Variations in food availability are likely to prompt variations in food intakes (calories and nutrients), which are fundamental to satisfy cellular maintenance, thermoregulation and locomotion costs [45, 142]; these ecological processes have the potential to directly affect species' diel activity rhythm [105,255,272,367]. A great number of mammals living in seasonally changing environment are doubtlessly seasonal breeders [294]. Two well-known seasonal predictors that prepare individuals metabolically for breeding are photoperiodism and secondary plant compounds found in newly emerging vegetation [97]. It is likely to observe variations of the diel activity rhythm of species during the course of pregnancy and nursing [372].

2.5.3 Profiling seasonal shifts

Seasonal shifts in diel activity rhythm varied in their amplitude and direction among species. Comparing the amplitude of species' seasonal shift with each other must be done carefully because their significance depends on the overall versatility of the diel activity rhythm, which might vary greatly among species (Fig. 2.10). Nineteen species showed a significant shift in clock-timed

diel activity rhythm between winter and summer, and for 15 of them, this shift could not solely be explained by photoperiodism alignment (Table 2.3). Although the analysis also showed a significant seasonal shift in diel activity rhythm after annual daylength standardisation ($P'_{,s} < 0.05$) for three other species – aardvark, Cape hare and red hartebeest – it would be misleading to attempt to interpret its meaning since the clock-timed seasonal shift was not significant ($P_{,s} > 0.05$). Following clock-time, these three species showed a significant seasonal shift, which was induced by the pre-processing of time t in order to achieve daylength standardisation.

The hourly rhythm variation ($\text{LRV}'_{,s}$) reached its highest rate during different daily time periods θ depending on the species. This time period is likely to depend on the species' temporal preferences. For example, rock hyrax and klipspringer were the two species having their hourly rhythm variation reach its highest rate during the brightest hours of the 24-hour cycle (ϕ_d). These two species also allocate a considerable amount (more than 50%) of their daily activity to ϕ_d; in Chapter 3 section 3.4, rock hyrax and klipspringer are defined as diurnal species. As for Hewitt's red rock rabbit and Cape porcupine, defined as nocturnal species, their hourly rhythm variation reached its highest rate during the darkest hours of the daily cycle (ϕ_n).

In the case of no hourly rhythm variation observed ($\text{LRV}'_{,s}(\theta) = 0$), it was either because species s had not shifted its proportions of daily activity throughout this time period, or that species s was not active at all in both summer and winter, throughout this time period (e.g. Hewitt's red rock rabbit during the brightest hours of the day, Table 2.2).

However, nine of the 15 species, eland, caracal, scrub hare, steenbok, Cape gray mongoose, grey duiker, black-backed jackal, chacma baboon and gemsbok, had their hourly rhythm variation reach its highest rate during the crepuscular hours (ρ) of the 24-hour cycle, independently of their temporal preferences. This supports the idea that photoperiodism plays a crucial role in the adjustment of mammal diel activity rhythms in the Little Karoo.

Among the 15 mammal species that showed a significant change of their seasonal diel activity rhythms both before and after daylength standardisation, 10 shifted proportions of their daily activity from warmer daily time periods to cooler ones, in summer compared to winter. Most of the activity shifts went from the brightest and evening crepuscular hours (ϕ_d and ρ_e) towards morning crepuscular hours (ρ_m, and to a lesser extent towards the darkest hours ϕ_n). This trend could be the result of a behavioural strategy to avoid hot midday and evening hours, and consequently minimise time exposure to a physiologically stressful environment caused by high temperatures

in summer (Fig. 2.13) [113, 150, 157, 158, 201, 336]. Besides the thermoregulatory benefits of restricting activities to cooler time periods, it offers the opportunity to increase the water intake by feeding at night or before dawn when dew forms on vegetation [334]. It is less explicit to interpret the significant shift of daily activity from dark night (ϕ_n) towards morning twilight (ρ_m), which was observed between winter and summer for Hewitt's red rock rabbit, scrub hare, black-backed jackal and gemsbok. The NMDS analysis represented these four species close to one another in Fig. 2.11, suggesting little dissimilarity was observed between their seasonal shifts in diel activity rhythm.

The 4% increase of the proportions of daily activity allocated to ϕ_d by the mammal community c in summer – despite the opposite behaviour followed by most of the species within c, except red hartebeest and chacma baboon – was due to the large weight that species chacma baboon had in c. With 1,514 independent photo-capture events collected for chacma baboon over winter and summer together, the species had a 17% weight in c, compared to 4% in $\bar{c}$, where all 25 mammal species received equal weight.

Changes in timing of the diel activity rhythm of 25 mammal species between winter and summer, resulted into a shift in the proportions of the daily activity of community $\bar{c}$ from the brightest and evening crepuscular hours (ϕ_d and ρ_e) towards morning crepuscular hours ρ_m, supporting furthermore the behavioural strategy leading to a reduction of time exposure to a physiologically stressful environment caused by high temperatures in summer. Although the study registered information for each season over two consecutive years, it might not be sufficient to determine stability of versatilities within seasons with respect to different years.

2.6 Tables

Table 2.1: Bootstrapped p-values
The Nw and Ns are respectively the number of photo-capture events collected across winter and summer for 25 mammal species in the Little Karoo; $O_{,s}$, $O^{'}_{,s}$ and $O^{''}_{,s}$ (built with t, $t^{'}$ and $t^{''}$) are the overlap coefficients between winter and summer diel activity rhythms; $P_{,s}$, $P^{'}_{,s}$ and $P^{''}_{,s}$ are the bootstrapped p-values (in %) showing whether winter and summer diel activity rhythms are significantly different ($< 5\%$).

Species	Nw	Ns	$O_{,s}$	$P_{,s}$	$O^{'}_{,s}$	$P^{'}_{,s}$	$O^{''}_{,s}$	$P^{''}_{,s}$
aardvark	81	55	0.84	10	0.81	**3**	0.84	11
aardwolf	42	68	0.57	**0**	0.57	**0**	0.57	**0**
African wildcat	261	130	0.82	**0**	0.88	15	0.82	**0**
black backed jackal	484	362	0.82	**0**	0.86	**0**	0.81	**0**
brown hyena	50	23	0.80	18	0.81	22	0.79	18
Cape gray mongoose	229	73	0.70	**0**	0.81	**0**	0.70	**0**
Cape hare	23	69	0.81	18	0.76	5	0.81	15
Cape mountain zebra	37	48	0.67	**1**	0.80	49	0.69	**3**
Cape porcupine	178	187	0.76	**0**	0.81	**0**	0.77	**0**
caracal	226	80	0.68	**0**	0.80	**0**	0.68	**0**
chacma baboon	521	993	0.84	**0**	0.87	**0**	0.84	**0**
eland	173	143	0.67	**0**	0.74	**0**	0.67	**0**
gemsbok	426	372	0.82	**0**	0.88	**0**	0.81	**0**
greater kudu	153	90	0.78	**0**	0.89	76	0.78	**0**
grey duiker	362	644	0.70	**0**	0.85	**0**	0.70	**0**
grey rhebuck	62	111	0.82	11	0.85	30	0.82	9
Hewitts red rock rabbit	30	32	0.67	**1**	0.72	**4**	0.72	6
honey badger	44	32	0.54	**0**	0.66	**1**	0.56	**0**
klipspringer	167	136	0.73	**0**	0.80	**0**	0.74	**0**
leopard	95	81	0.69	**0**	0.84	17	0.71	**0**
red hartebeest	30	118	0.78	22	0.69	**1**	0.77	21
rock hyrax	17	33	0.36	**0**	0.46	**0**	0.36	**0**
scrub hare	327	81	0.82	**1**	0.80	**0**	0.85	7
springbok	20	55	0.69	9	0.72	19	0.69	9
steenbok	121	93	0.66	**0**	0.80	**4**	0.67	**0**

Community	Nw	Ns	$O_{,c}$	$P_{,c}$	$O^{'}_{,c}$	$P^{'}_{,c}$	$O^{''}_{,c}$	$P^{''}_{,c}$
c	4159	4109	0.88	**0**	0.87	**0**	0.88	**0**
$\bar{c}$ (equal weight)	-	-	0.83	**0**	0.89	**0**	0.83	**0**

Table 2.2: Seasonal shift in diel activity rhythm
(Caption on following page)

	$\text{TRV}'_{,s}$	$\text{LRV}'_{,s}$					$\text{LAS}'_{,s}$					$I'_{,s}$				
Species	24-h cycle	ρ_m	ϕ_d	ρ_e	ϕ_n	ρ	ρ_m	ϕ_d	ρ_e	ϕ_n	ρ	ρ_m	ϕ_d	ρ_e	ϕ_n	ρ
rock hyrax *	54	40	53	5	2	*45*	45	-49	4	0	*49*	1	1	1	1	*1*
aardwolf *	43	13	2	21	64	*34*	9	1	-20	10	*-11*	1	1	1	5	*2*
honey badger *	34	18	8	22	52	*40*	-11	-6	-19	36	*-30*	1	1	1	1	*1*
red hartebeest *	31	25	32	13	30	*38*	6	19	-13	-12	*-7*	2	1	1	1	*3*
Hewitts red rock rabbit *	28	24	0	10	65	*34*	18	0	-3	-15	*15*	1	NA	2	2	*1*
springbok	28	21	43	7	29	*28*	8	-18	-5	15	*3*	1	1	1	1	*5*
eland *	26	23	14	32	31	*55*	13	-5	-21	13	*-8*	1	2	1	1	*3*
Cape hare *	24	13	0	10	76	*23*	8	0	6	-14	*14*	1	NA	1	2	*1*
Cape mountain zebra	20	17	25	21	37	*38*	2	-11	-8	17	*-6*	4	1	1	1	*2*
caracal *	20	11	20	29	40	*40*	7	-7	-13	13	*-6*	1	1	1	1	*2*
klipspringer *	20	18	42	26	14	*44*	8	0	-12	4	*-4*	1	202	1	1	*4*
scrub hare *	20	36	6	9	49	*45*	9	1	2	-12	*11*	1	2	2	2	*1*
steenbok *	20	42	21	10	27	*52*	1	-4	5	-2	*5*	22	2	1	6	*4*
aardvark *	19	24	0	4	71	*28*	13	0	2	-15	*15*	1	NA	1	2	*1*
brown hyena	19	3	0	13	83	*16*	4	0	9	-13	*13*	1	NA	1	2	*1*
Cape gray mongoose *	19	46	26	22	6	*68*	17	-10	-8	1	*9*	1	1	1	1	*3*
Cape porcupine *	19	17	4	13	66	*30*	6	1	-7	0	*-1*	1	2	1	287	*16*
leopard	16	23	6	14	57	*37*	-7	-2	-8	17	*-15*	1	1	1	1	*1*
grey duiker *	15	44	26	8	22	*52*	6	-7	-1	2	*6*	2	1	4	6	*3*
grey rhebuck	15	39	24	6	31	*45*	14	-3	-4	-7	*10*	1	3	1	1	*1*
black-backed jackal *	14	51	14	7	28	*58*	15	-4	-2	-9	*13*	1	1	1	1	*1*
chacma baboon *	13	15	44	38	3	*53*	3	7	-10	0	*-7*	2	2	1	9	*2*
African wildcat	12	23	11	32	34	*55*	7	0	-5	-2	*2*	1	97	1	5	*7*
gemsbok *	12	29	20	20	31	*49*	8	2	-5	-5	*3*	1	3	1	1	*4*
greater kudu	11	32	20	12	36	*44*	10	-6	3	-7	*13*	1	1	1	1	*1*
	TRV'	LRV'					LAS'					I'				
Community	24-h cycle	ρ_m	ϕ_d	ρ_e	ϕ_n	ρ	ρ_m	ϕ_d	ρ_e	ϕ_n	ρ	ρ_m	ϕ_d	ρ_e	ϕ_n	ρ
c	15	34	17	18	31	*52*	8	4	-4	-8	*4*	1	1	1	1	*3*
$\bar{c}$ (equal weight)	15	34	19	21	26	*60*	8	-3	-5	0	*3*	1	1	1	11	*4*

Table 2.2: Seasonal shift in diel activity rhythm

All descriptive statistics, provided above for 25 mammal species in the Little Karoo, were calculated after annual daylength standardisation of the data (t'). * is showing next to the names of species with a significant seasonal change ($P'_{,s} < 0.05$). $\text{TRV}'_{,s}$ represents the total rhythm variation of species s between winter and summer, which also consists of the percentage of diel activity rhythm that shifted between the two seasons. Time of day was divided into four θ time periods: ρ_m, ϕ_d, ρ_e and ϕ_n ($\rho = \rho_m + \rho_e$, showing in italic). $\text{LRV}'_{,s}(\theta)$ provides the local rhythm variation of species s during time period θ, which consists of the percentage of $\text{TRV}'_{,s}$ explained during θ. Divided by the number of hours in θ, the local rhythm variation highlighted the daily time period that explained most of the $\text{TRV}'_{,s}$ per hour, for species s; it was shaded in gray. $\text{LAS}'_{,s}(\theta)$ represents the local activity shift of species s during time period θ, which consists of the resulting shift in daily activity proportions allocated by species s throughout θ. All substantial increases ($> 2\%$) of the proportions of daily activity in summer, were highlighted in orange, whereas all substantial decreases ($< -2\%$) were highlighted in blue. Finally, $I'_{,s}(\theta)$ represents the compensation index of species s during time period θ, which equaled 1 when $\text{LRV}'_{,s}(\theta)$ was entirely converted into a shift in activity. However, when compensation effects (activity increases compensated by activity decreases throughout θ) occurred, $I'_{,s}(\theta)$ took values greater than one. When a species showed no activity during θ in both seasons, the associated $\text{LRV}'_{,s}(\theta)$ and $\text{LAS}'_{,s}(\theta)$ equaled 0, and $I'_{,s}(\theta)$ returned NA.

TRV', LRV', LAS' and I' apply similarly to the mammal community c and $\bar{c}$ as a whole.

Reading example: 54% of rock hyrax's diel activity rhythm shifted between winter and summer. Most of the shift took place during ρ_m (40%) and ϕ_d (53%) periods of the 24-hour cycle. In summer, rock hyrax increased by 45% the proportion of its daily activity allocated to ρ_m, whereas it decreased by 49% the proportion of its daily activity allocated to ϕ_d. The seasonal shift in activity primarily went from ϕ_d to ρ_m.

For Cape porcupine, 66% of the seasonal shift took place during ϕ_n. However, the resulting activity shift during ϕ_n was close to 0%, which was highlighted by $I'_{,s}(\phi_n) = 287$, ameaning that throughout ϕ_n, the activity increases were compensated by symmetric activity decreases.

Most of the total rhythm variation of the caracal took place during ϕ_n (40%). However, during ρ_e, the extent of rhythm variation explained per hour, was greater and shaded in gray.

Table 2.3: Summary

For 25 mammal species in the Little Karoo: $O_{,s}$ and $O^{'}_{,s}$ (built with t and $t^{'}$) are the overlap coefficients between winter and summer diel activity rhythms; $P_{,s}$ and $P^{'}_{,s}$ are the associated bootstrapped p-values and * indicates a significant seasonal change (< 0.05); Ph indicates photoperiodism alignment and F indicates the influence of other factors.

Species	$O^{'}_{,s} - O_{,s}$	$P_{,s}$	$P^{'}_{,s}$	Ph	F
African wildcat	+	*		x	
Cape mountain zebra	+	*		x	
greater kudu	+	*		x	
leopard	+	*		x	
aardwolf	=	*	*		x
black backed jackal	+	*	*	(x)	x
Cape gray mongoose	+	*	*	(x)	x
Cape porcupine	+	*	*	(x)	x
caracal	+	*	*	(x)	x
chacma baboon	+	*	*	(x)	x
eland	+	*	*	(x)	x
gemsbok	+	*	*	(x)	x
grey duiker	+	*	*	(x)	x
Hewitts red rock rabbit	+	*	*	(x)	x
honey badger	+	*	*	(x)	x
klipspringer	+	*	*	(x)	x
rock hyrax	+	*	*	(x)	x
scrub hare	–	*	*		x
steenbok	+	*	*	(x)	x
aardvark	–		*		
Cape hare	–		*		
red hartebeest	–		*		
brown hyena	+			(x)	
grey rhebuck	+			(x)	
springbok	+			(x)	

2.7 Figures

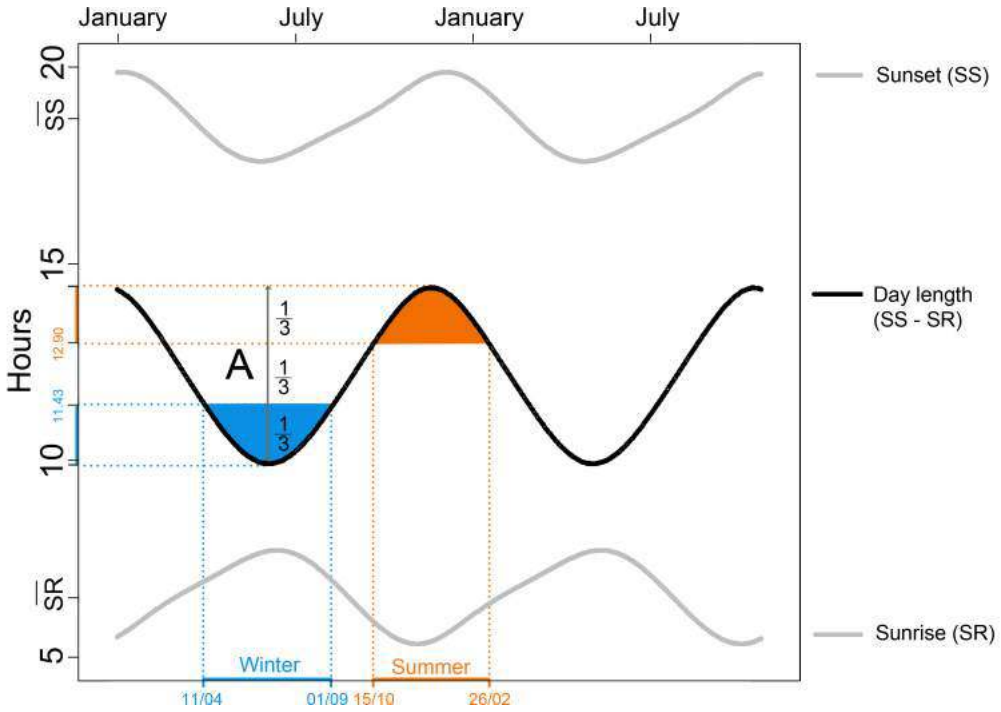

Figure 2.1: Daylength oscillations throughout the year, in the Little Karoo
Winter is defined as the period of the year with daylength D_l varying within the bottom third of its annual range A ($D_l < 11.43$), and summer as the period of the year with daylength varying within the top third ($D_l > 12.90$). Consequently, winter starts on 11 April and ends on 01 September, whereas summer starts on 15 October and ends on 26 February.

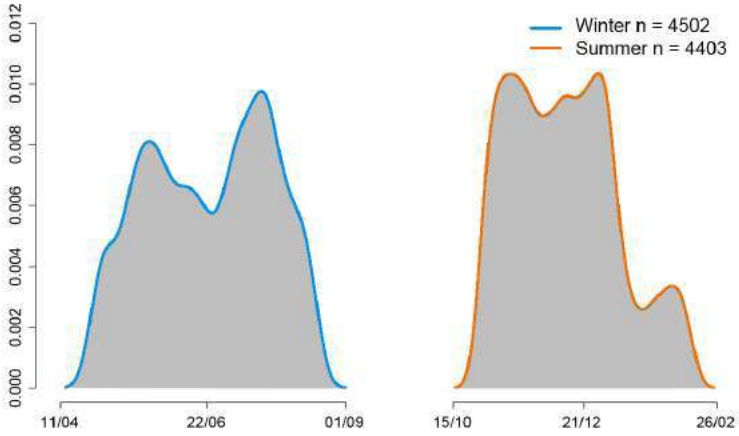

Figure 2.2: Data collection in winter and summer
The graph shows the distributions of the number of photo-captures collected in winter and in summer, in the Little Karoo.

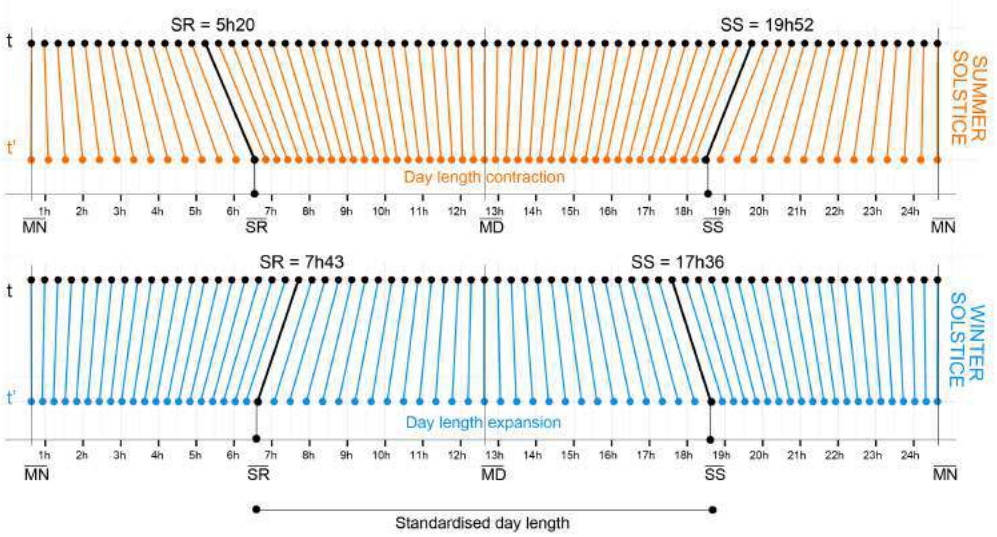

Figure 2.3: Daylength standardisation ($t^{'}$)
Pre-processing of t on the days of the southern winter and summer solstices. In summer and winter, the time variable t gets distorted in opposite ways, resulting into a standardisation of daylength to 12 hours, throughout the year. Independently on the date T of the year (except on the days of the equinoxes), the adjustment ($|t^{'} - t|$) is always greatest at sunrise ($t = SR$) and at sunset ($t = SS$).

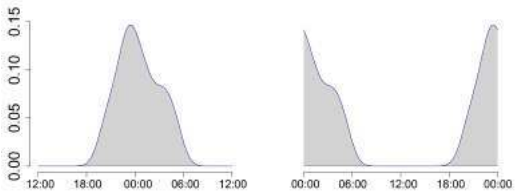

(a) Effect of time origin: midnight vs noon

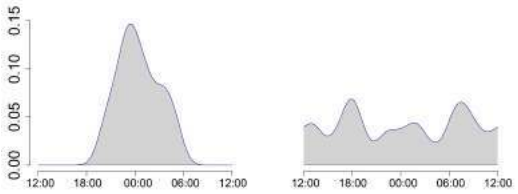

(b) Unimodal and symmetric distribution assumptions

Figure 2.4: The problems of circular data
(a) The aardvark diel activity rhythm appears either as a unimodal or a U-shaped distribution, whether the display is centred around midnight or around noon. (b) The aardvark diel activity rhythm (left density function) follows a unimodal and symmetric circular distribution, contrarily to the multimodal diel activity rhythm of the greater kudu (right density function).

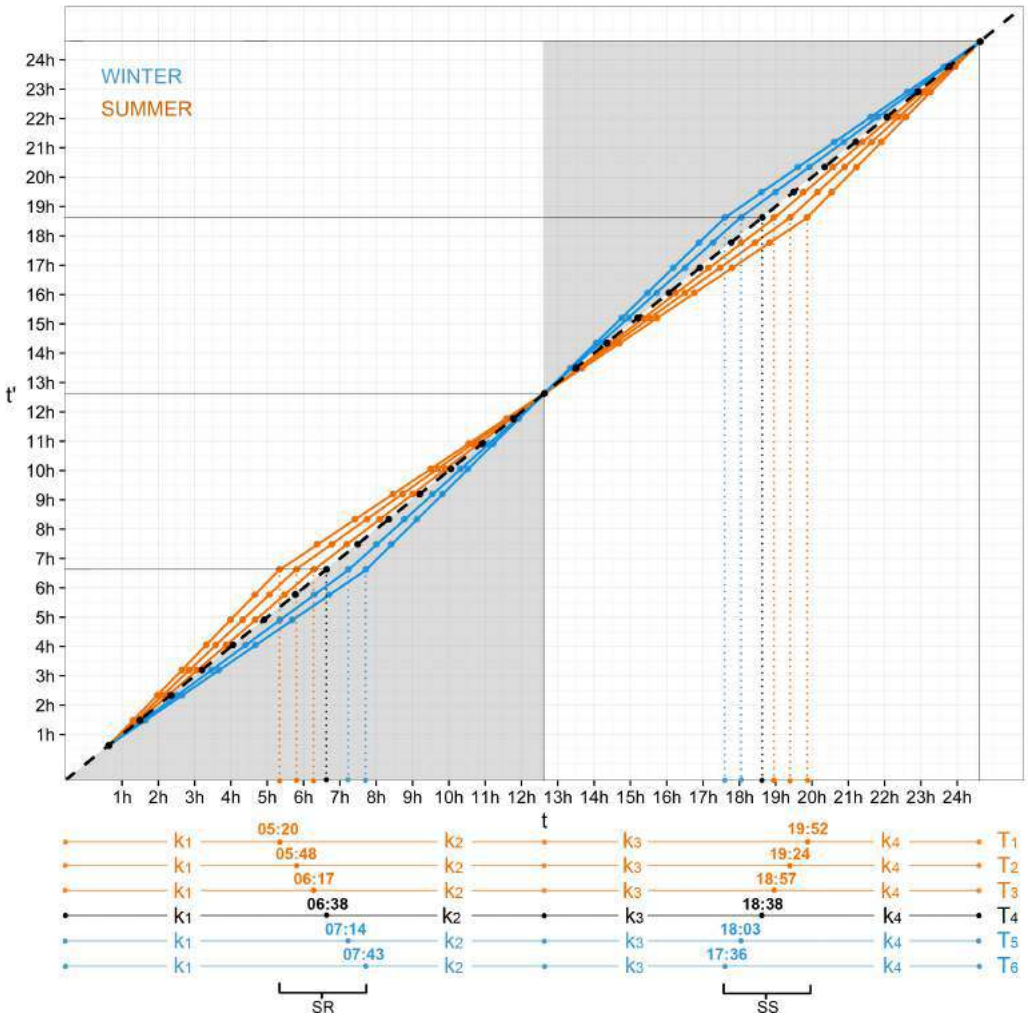

Figure 2.5: Pre-processing function f: $t^{'} = f(t, T)$

The graph shows the pre-processing of the time variable t, on six different days of the year (T), including on the vernal and fall equinoxes (T_4) as well as on the southern winter (T_6) and summer (T_1) solstices. f is defined by four equations with domain of definition depending on sunrise (SR) and sunset (SS) times, the latter depending themselves on T. On the days of the equinoxes ($SR = \overline{SR}$ and $SS = \overline{SS}$), therefore no adjustment was computed ($t^{'} = t$, black line). During winter mornings ($SR > \overline{SR}$), t was then adjusted to lower values ($t^{'} < t$, blue lines), and during winter afternoons ($SS < \overline{SS}$), t was adjusted to greater values ($t^{'} > t$, blue lines), resulting into an expansion of daylength (grey area). The opposite distortion took place in summer (orange lines), resulting into a contraction of daylength (white area).

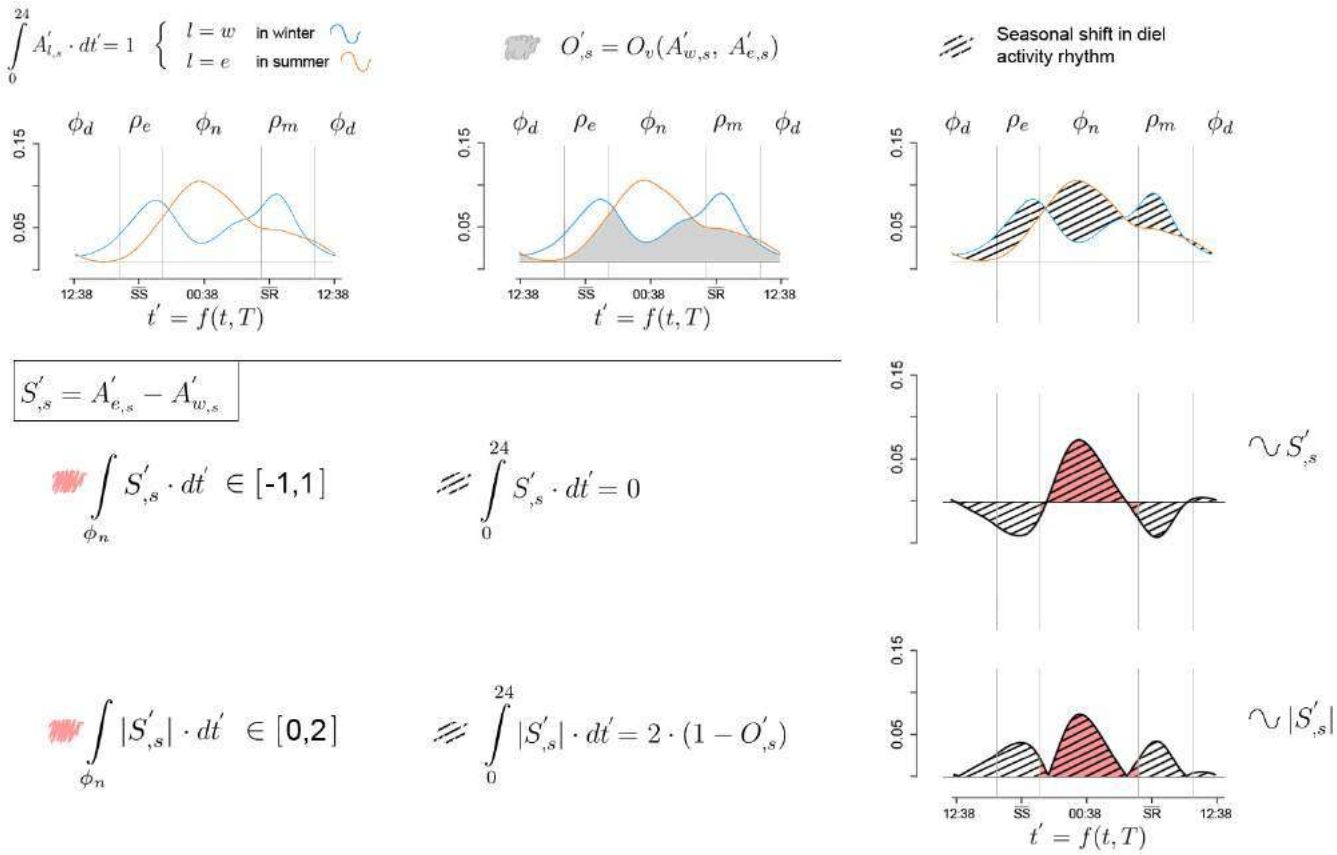

Figure 2.6: Mathematical relationships between $A'_{l,s}$, $O'_{,s}$ and $S'_{,s}$

$A'_{e,s}$ and $A'_{w,s}$ are the probability density functions representing the diel activity rhythms of species s in summer and winter. $O'_{,s}$ represents the area of overlap between the two probability density functions. Both $S'_{,s}$ and $|S'_{,s}|$ provide insights into the seasonal shift in diel activity rhythm of species s between summer and winter. $|S'_{,s}|$ illustrates the extent of the rhythm variation between summer and winter, whereas $S'_{,s}$ illustrates the resulting activity shift.

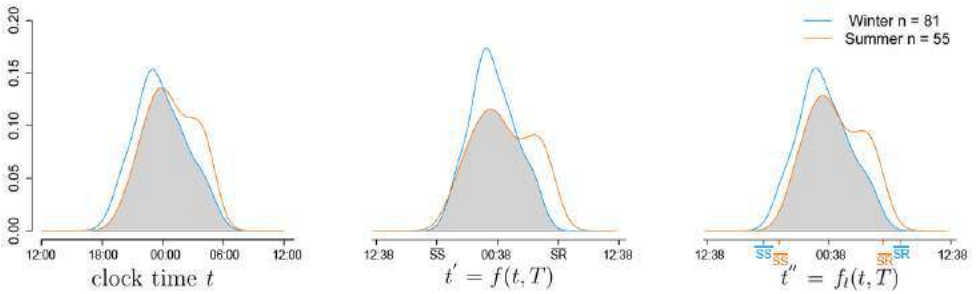

(a) Aardvark, midnight-centred diel activity rhythm

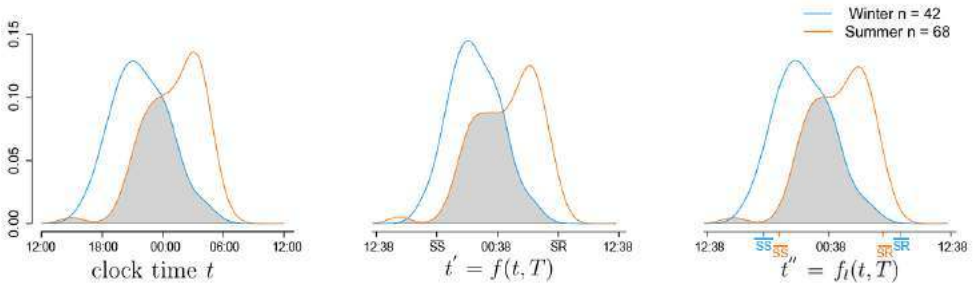

(b) Aardwolf, midnight-centred diel activity rhythm

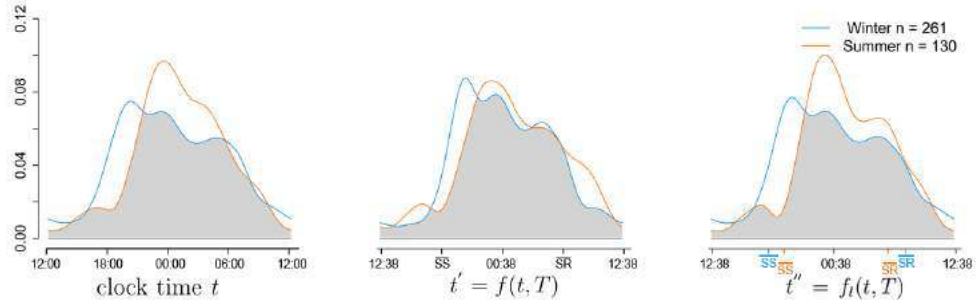

(c) African wildcat, midnight-centred diel activity rhythm

Figure 2.7: Species seasonal diel activity rhythms

Winter and summer diel activity rhythms are displayed for 25 mammal species s in the Little Karoo, using three different time metrics: traditional 24-hour human clock-time t and two ecological times with standardised sunrise and sunset times $t^{'}$ and $t^{''}$. The grey areas show the overlap between the two probability density functions in each plot, for summer and winter.

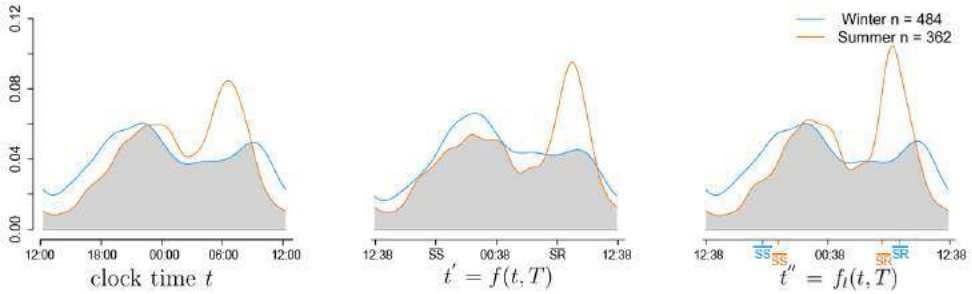

(d) black-backed jackal, midnight-centred diel activity rhythm

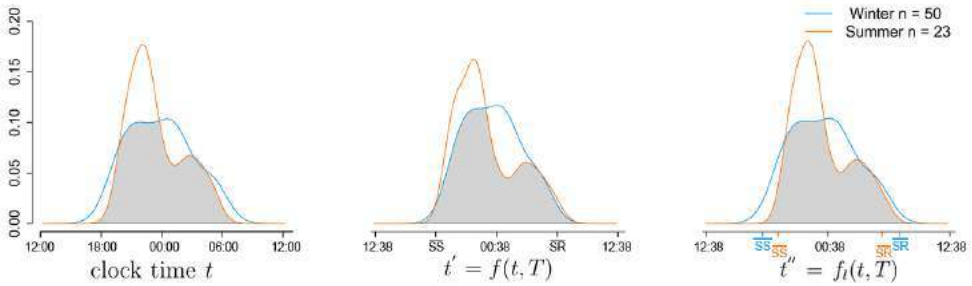

(e) Brown hyena, midnight-centred diel activity rhythm

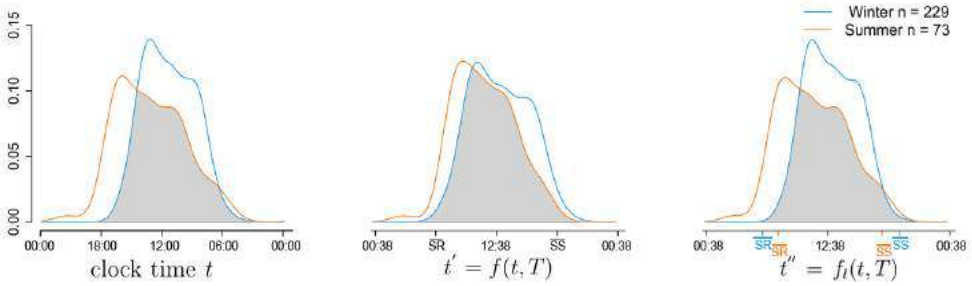

(f) Cape gray mongoose, noon-centred diel activity rhythm

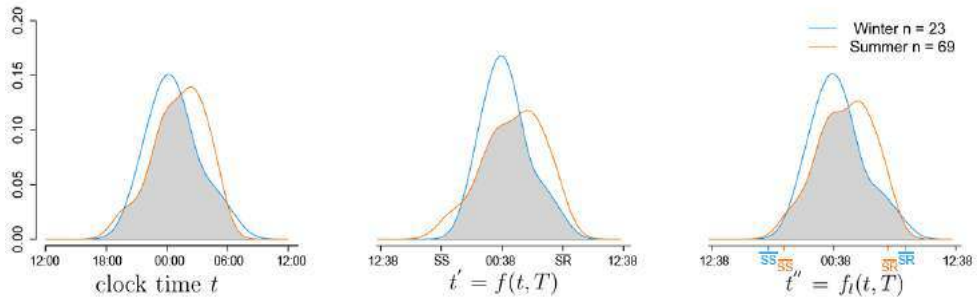

(g) Cape hare, midnight-centred diel activity rhythm

Figure 2.7: Seasonal shift in diel activity rhythms (continued)
A full caption is provided on p74.

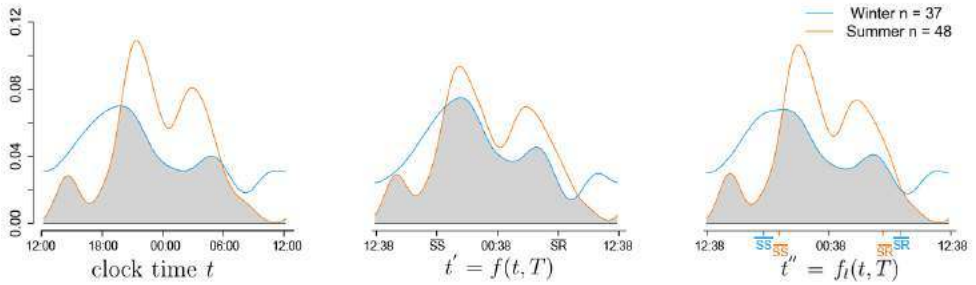

(h) Cape mountain zebra, midnight-centred diel activity rhythm

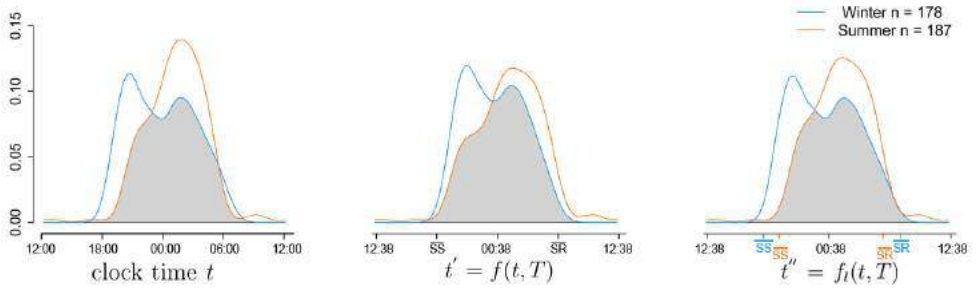

(i) Cape porcupine, midnight-centred diel activity rhythm

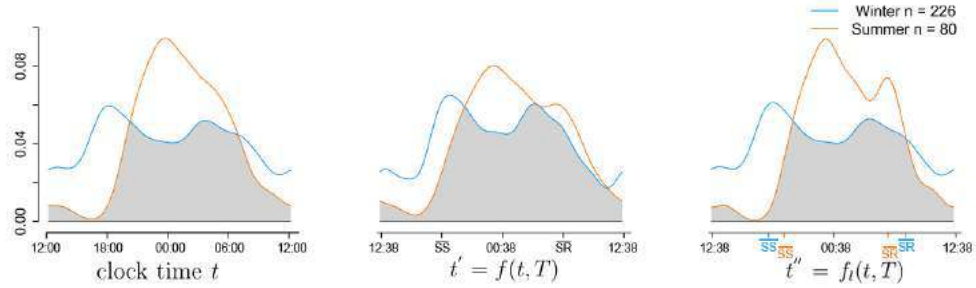

(j) Caracal, midnight-centred diel activity rhythm

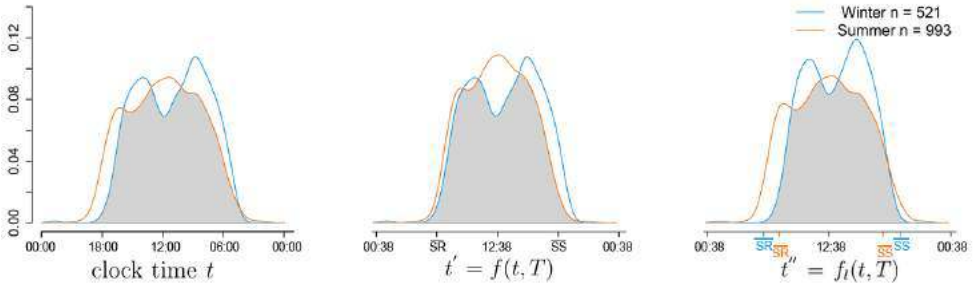

(k) Chacma baboon, noon-centred diel activity rhythm

Figure 2.7: Seasonal shift in diel activity rhythms (continued)
A full caption is provided on p74.

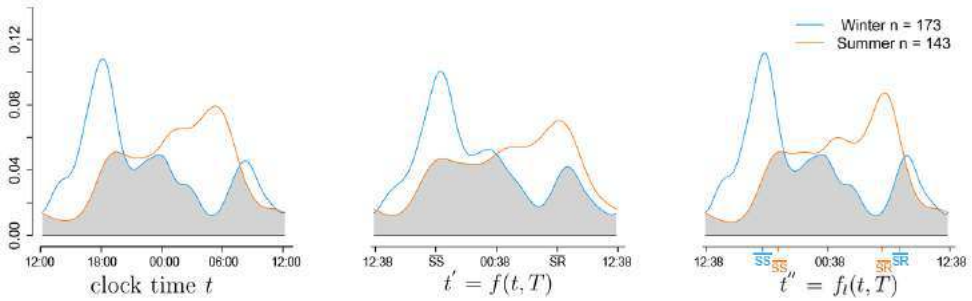

(l) Eland, midnight-centred diel activity rhythm

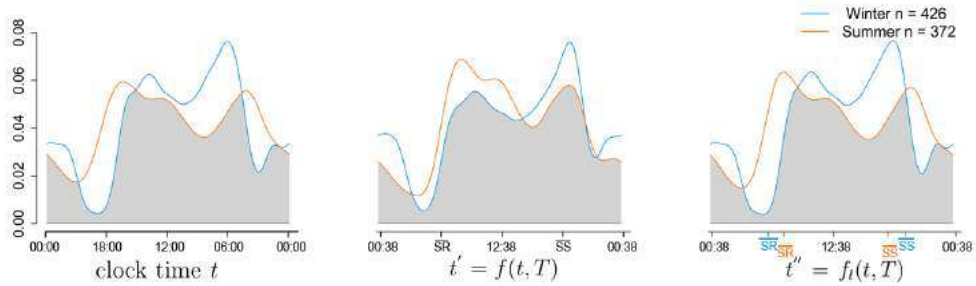

(m) Gemsbok, noon-centred diel activity rhythm

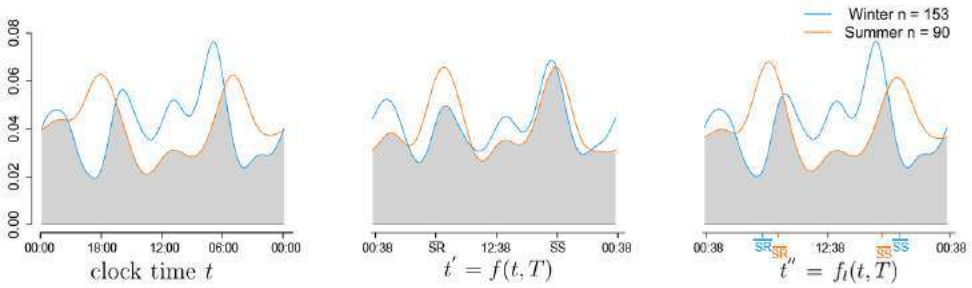

(n) Greater kudu, noon-centred diel activity rhythm

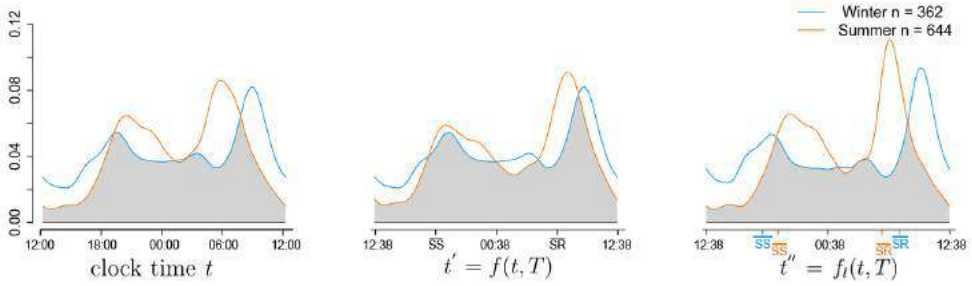

(o) Grey duiker, midnight-centred diel activity rhythm

Figure 2.7: Seasonal shift in diel activity rhythms (continued)
A full caption is provided on p74.

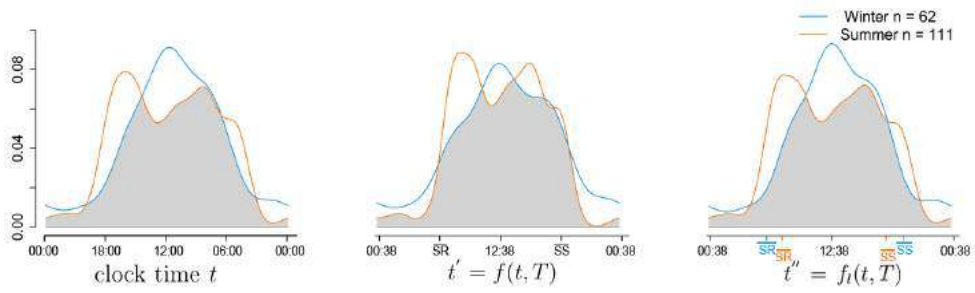

(p) Grey rhebuck, noon-centred diel activity rhythm

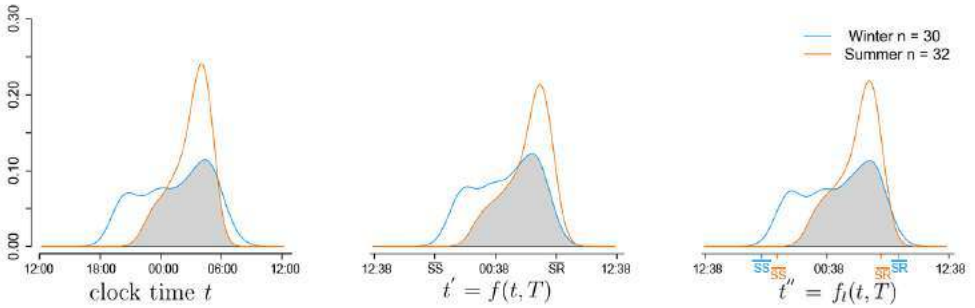

(q) Hewitt's red rock rabbit, midnight-centred diel activity rhythm

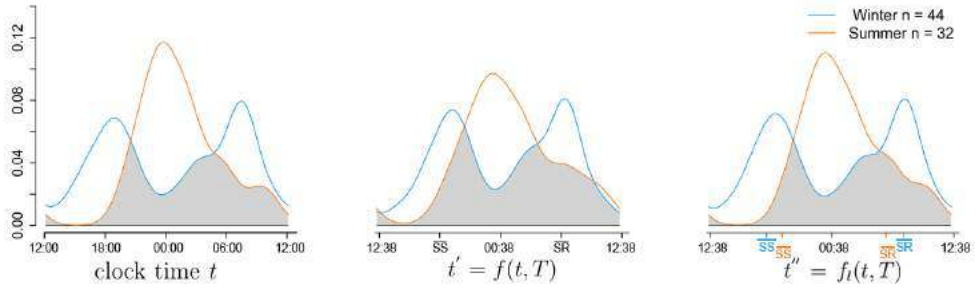

(r) Honey badger, midnight-centred diel activity rhythm

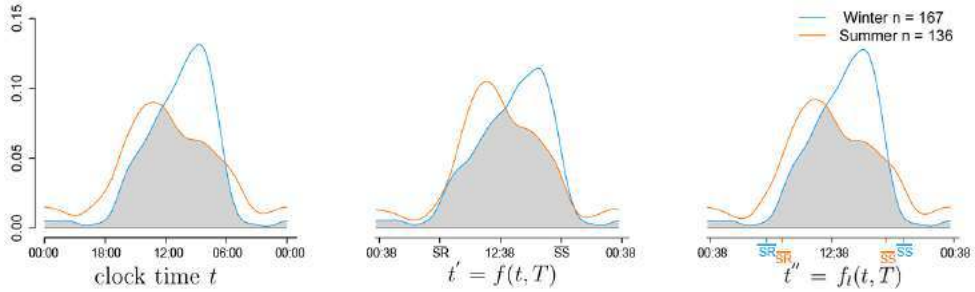

(s) Klipspringer, noon-centred diel activity rhythm

Figure 2.7: Seasonal shift in diel activity rhythms (continued)
A full caption is provided on p74.

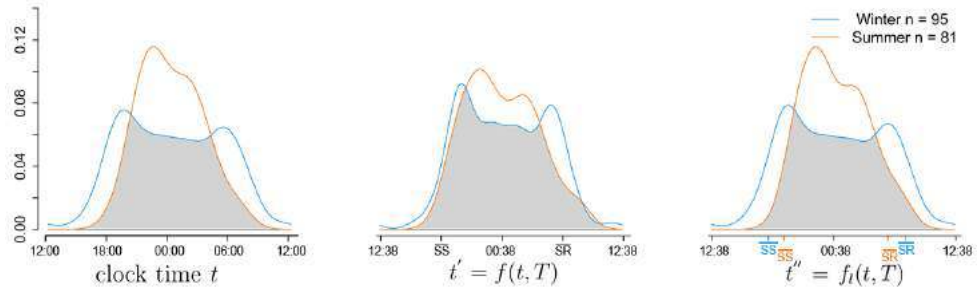

(t) Leopard, midnight-centred diel activity rhythm

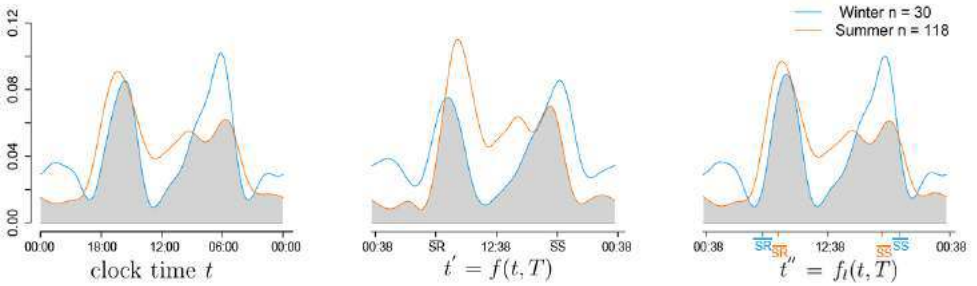

(u) Red hartebeest, noon-centred diel activity rhythm

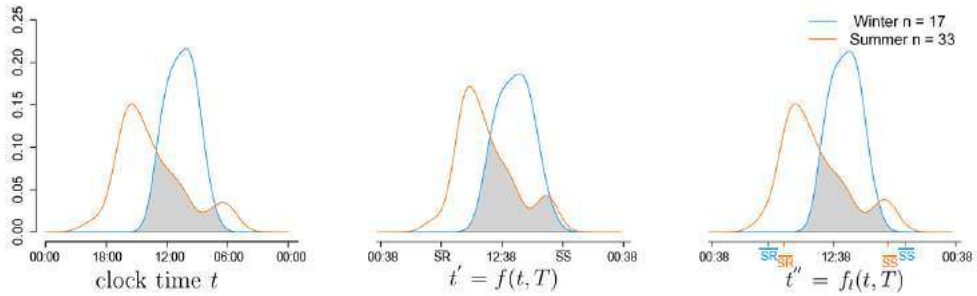

(v) Rock hyrax, noon-centred diel activity rhythm

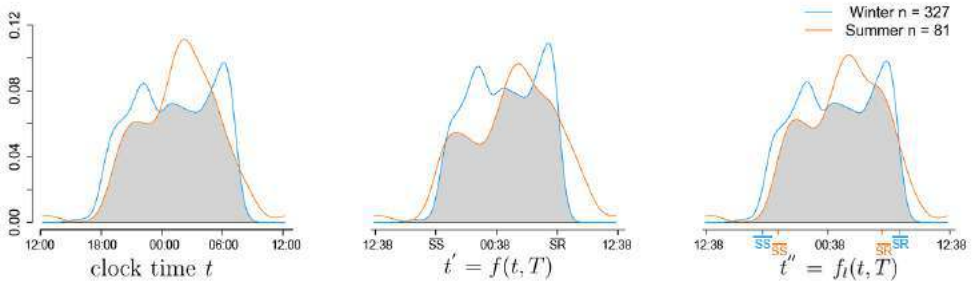

(w) Scrub hare, midnight-centred diel activity rhythm

Figure 2.7: Seasonal shift in diel activity rhythms (continued)
A full caption is provided on p74.

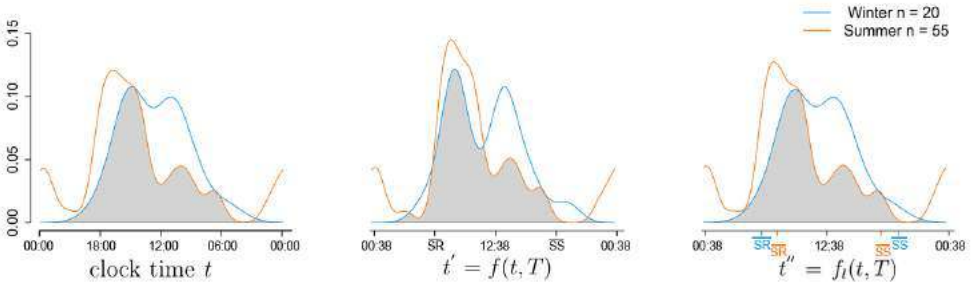

(x) Springbok, noon-centred diel activity rhythm

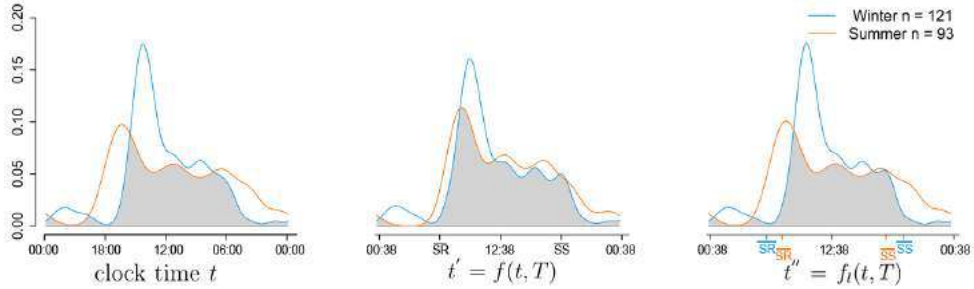

(y) Steenbok, noon-centred diel activity rhythm

Figure 2.7: Seasonal shift in diel activity rhythms (continued)
A full caption is provided on p74.

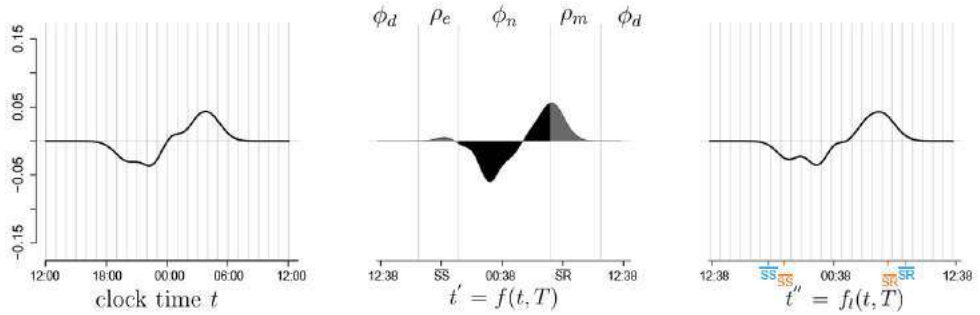

(a) Aardvark, midnight-centred diel activity rhythm

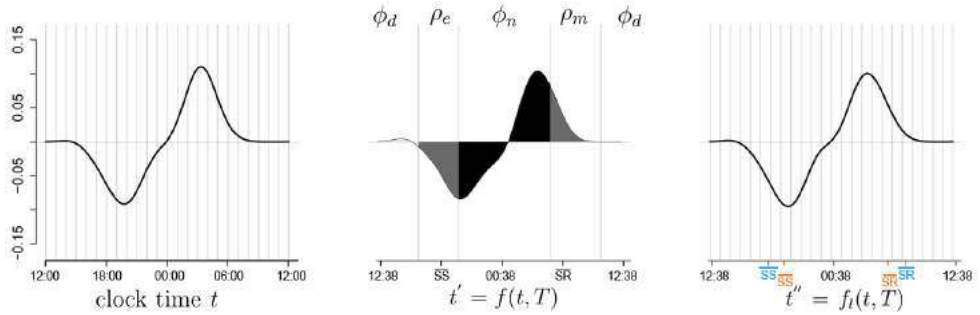

(b) Aardwolf, midnight-centred diel activity rhythm

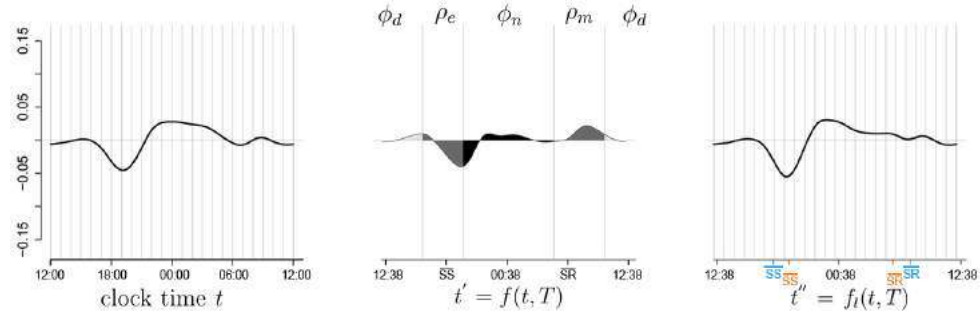

(c) African wildcat, midnight-centred diel activity rhythm

Figure 2.8: Seasonal shift in diel activity rhythms: summer − winter

The seasonal change in diel activity rhythms between summer and winter is quantified for 25 mammal species s in the Little Karoo, and in the three different time metrics: traditional 24-hour human clock-time t and two ecological times with standardised sunrise and sunset times $t^{'}$ and $t^{''}$. The functions $S_{,s}$, $S^{'}_{,s}$ and $S^{''}_{,s}$ are positive when the proportion of daily activity is higher in summer than in winter; vice versa for negative values.

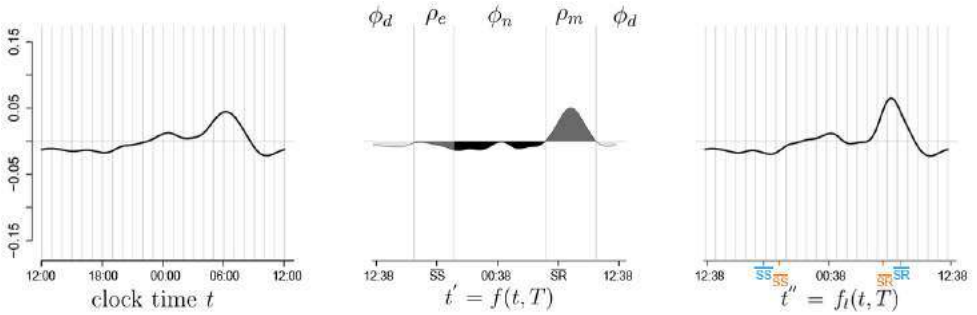

(d) black-backed jackal, midnight-centred diel activity rhythm

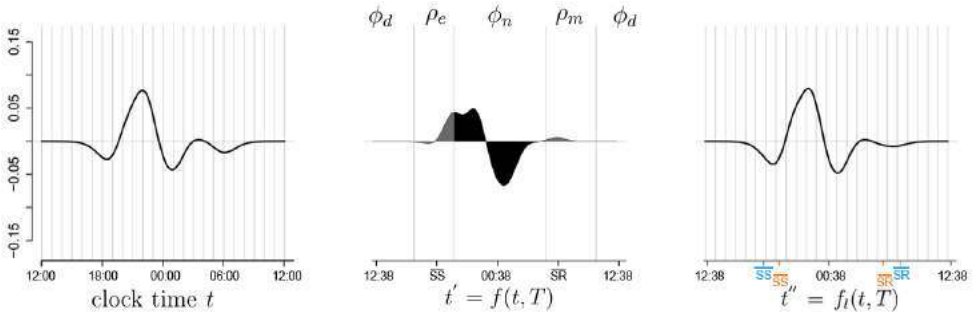

(e) Brown hyena, midnight-centred diel activity rhythm

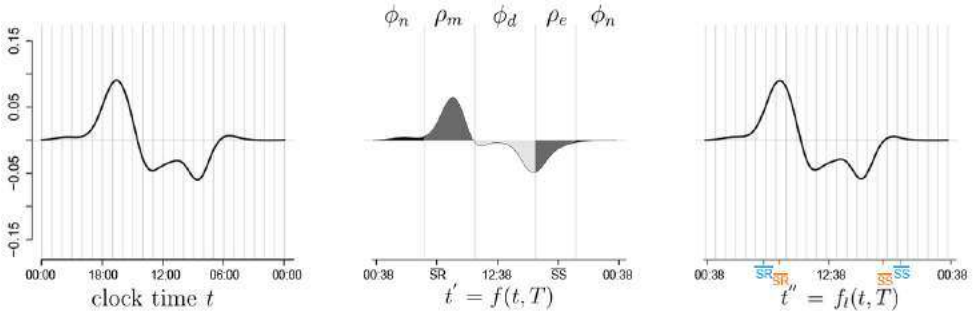

(f) Cape gray mongoose, noon-centred diel activity rhythm

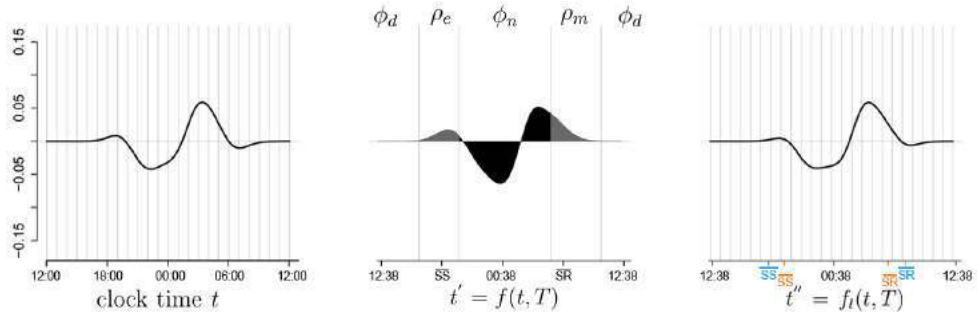

(g) Cape hare, midnight-centred diel activity rhythm

Figure 2.8: Seasonal shift in diel activity rhythms: summer − winter (continued)
A full caption is provided on p81.

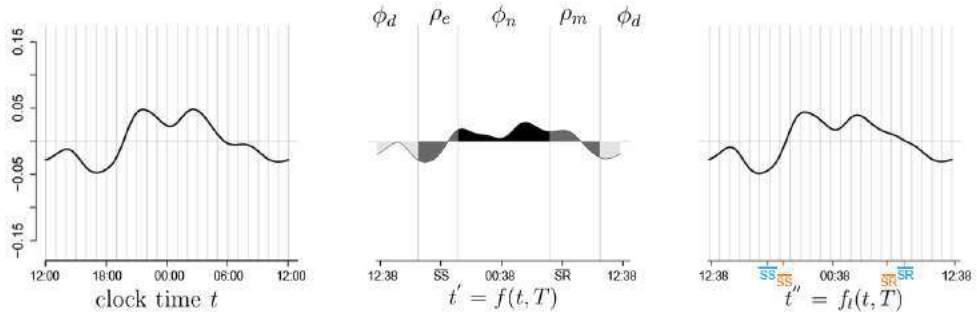

(h) Cape mountain zebra, midnight-centred diel activity rhythm

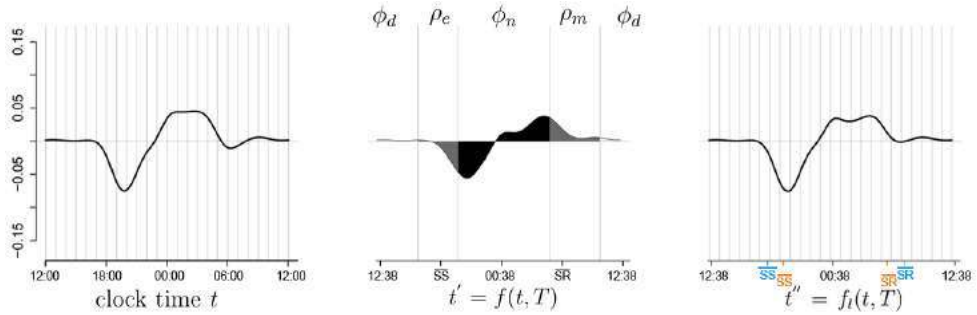

(i) Cape porcupine, midnight-centred diel activity rhythm

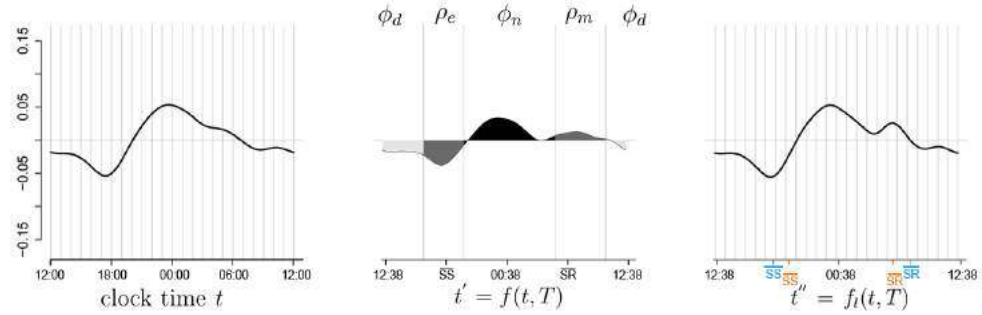

(j) Caracal, midnight-centred diel activity rhythm

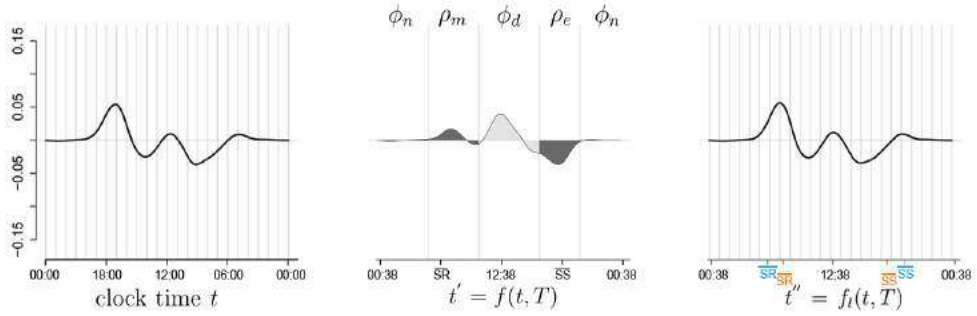

(k) Chacma baboon, noon-centred diel activity rhythm

Figure 2.8: Seasonal shift in diel activity rhythms: summer − winter (continued)
A full caption is provided on p81.

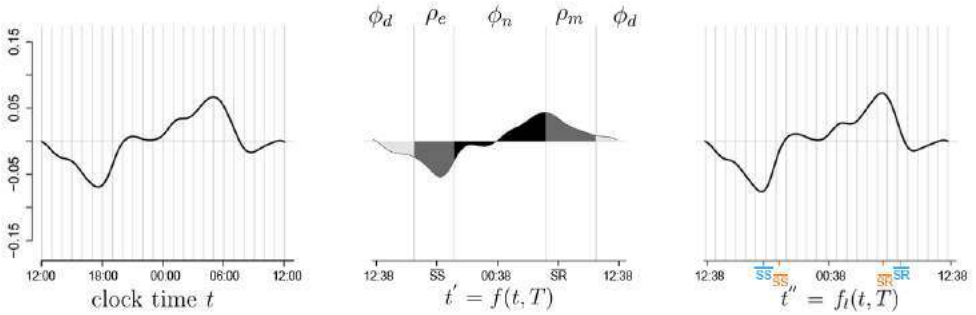

(l) Eland, midnight-centred diel activity rhythm

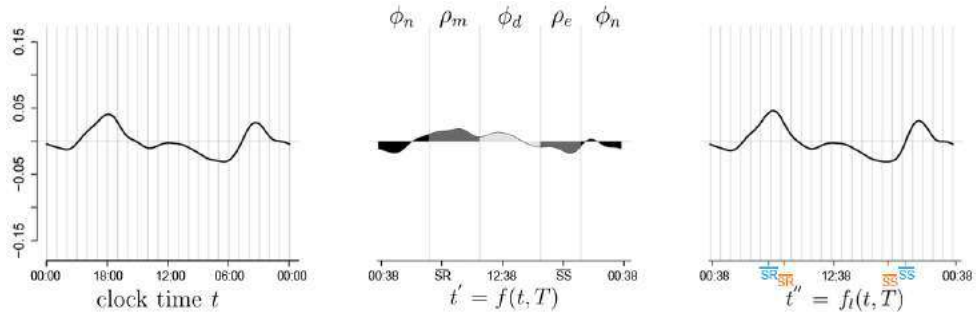

(m) Gemsbok, noon-centred diel activity rhythm

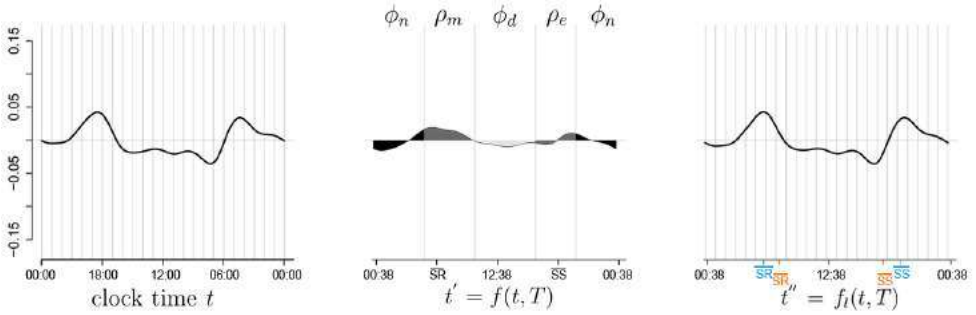

(n) Greater kudu, noon-centred diel activity rhythm

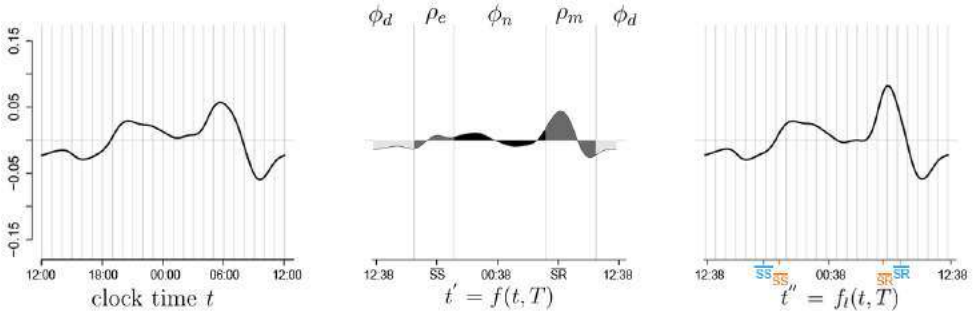

(o) Grey duiker, midnight-centred diel activity rhythm

Figure 2.8: Seasonal shift in diel activity rhythms: summer − winter (continued)
A full caption is provided on p81.

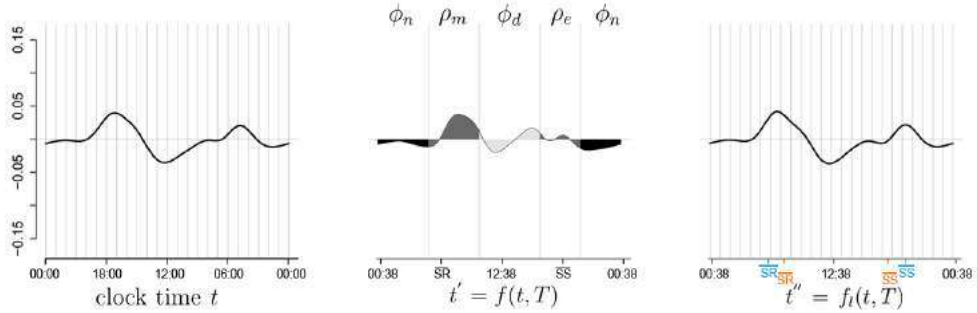

(p) Grey rhebuck, noon-centred diel activity rhythm

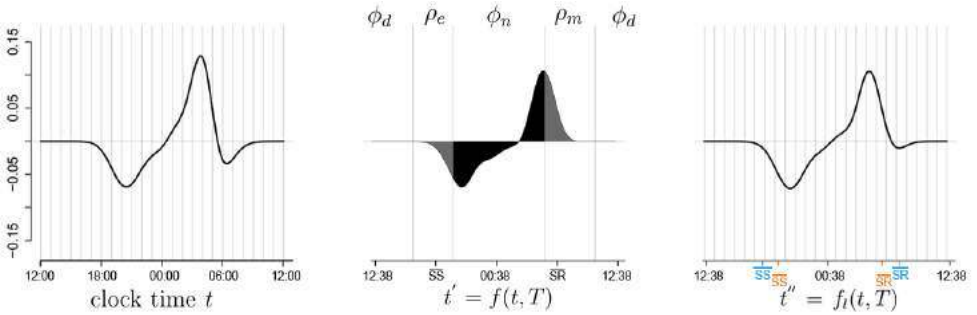

(q) Hewitt's red rock rabbit, midnight-centred diel activity rhythm

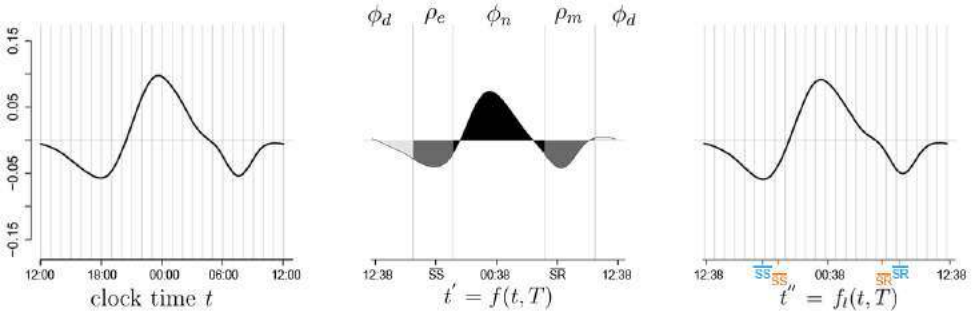

(r) Honey badger, midnight-centred diel activity rhythm

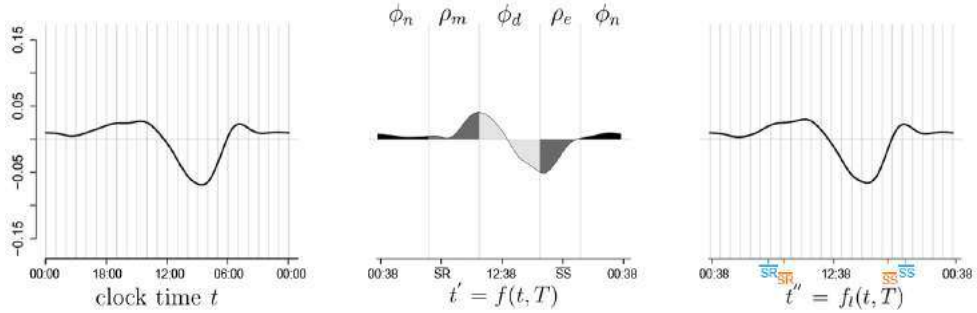

(s) Klipspringer, noon-centred diel activity rhythm

Figure 2.8: Seasonal shift in diel activity rhythms: summer − winter (continued)
A full caption is provided on p81.

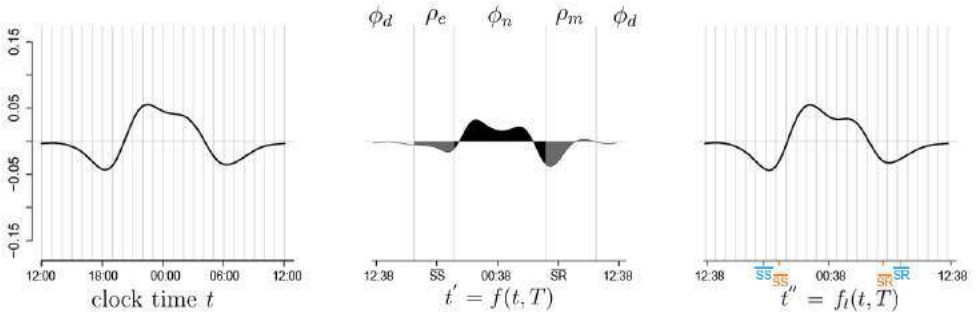

(t) Leopard, midnight-centred diel activity rhythm

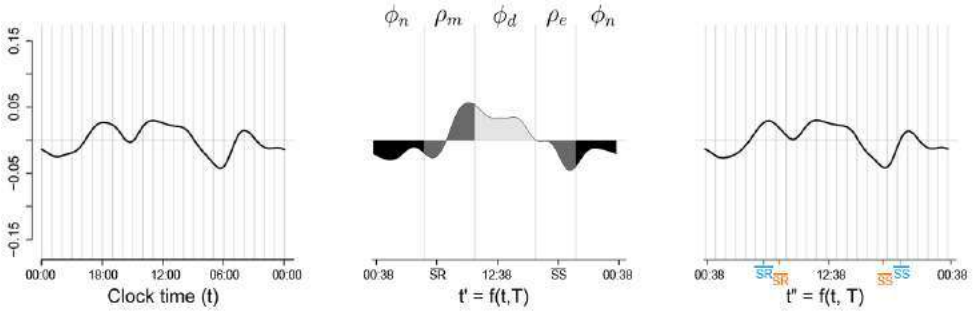

(u) Red hartebeest, noon-centred diel activity rhythm

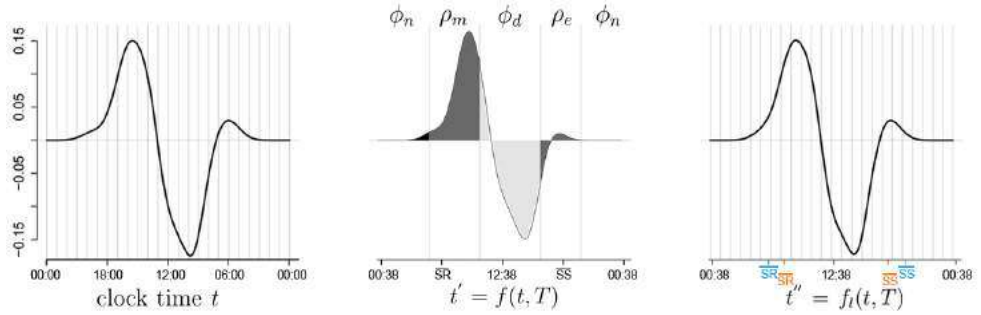

(v) Rock hyrax, noon-centred diel activity rhythm

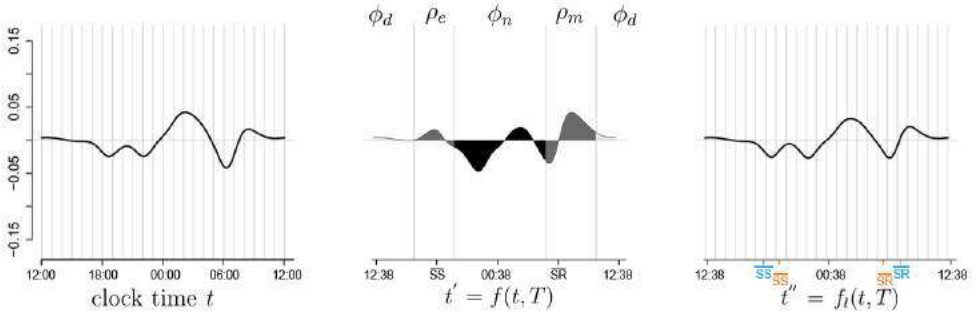

(w) Scrub hare, midnight-centred diel activity rhythm

Figure 2.8: Seasonal shift in diel activity rhythms: summer − winter (continued)
A full caption is provided on p81.

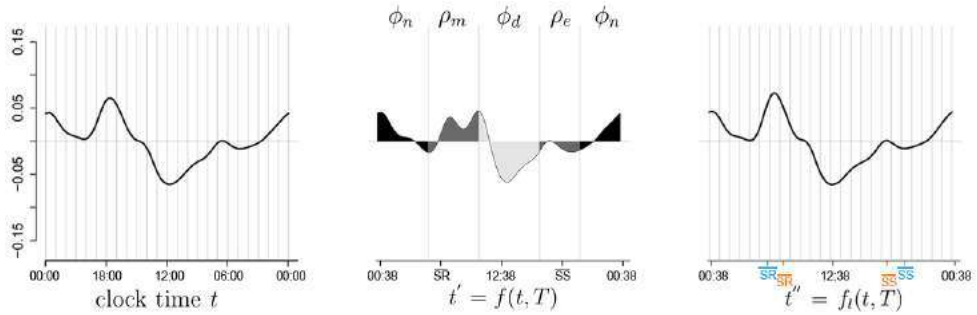

(x) Springbok, noon-centred diel activity rhythm

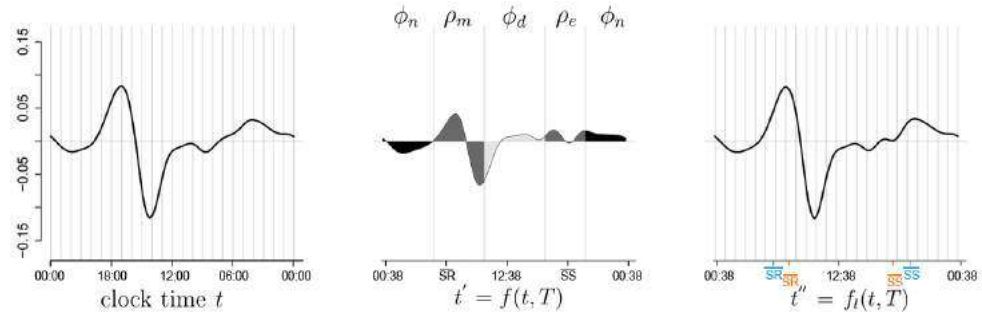

(y) Steenbok, noon-centred diel activity rhythm

Figure 2.8: Seasonal shift in diel activity rhythms: summer − winter (continued)
A full caption is provided on p81.

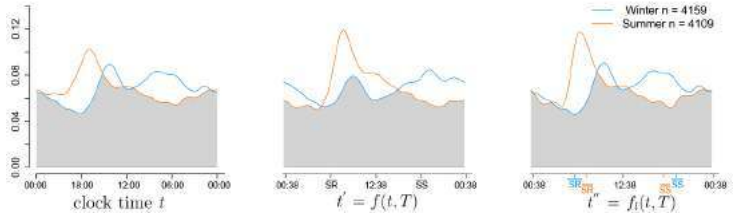

(a) Seasonal diel activity rhythms $A_{l,c}$, $A^{'}_{l,c}$ and $A^{''}_{l,c}$

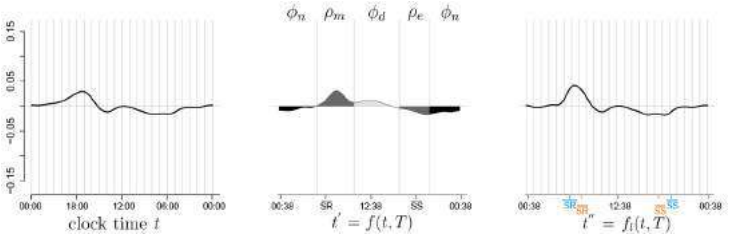

(b) Seasonal shift in diel activity rhythms $S_{,c}$, $S^{'}_{,c}$ and $S^{''}_{,c}$

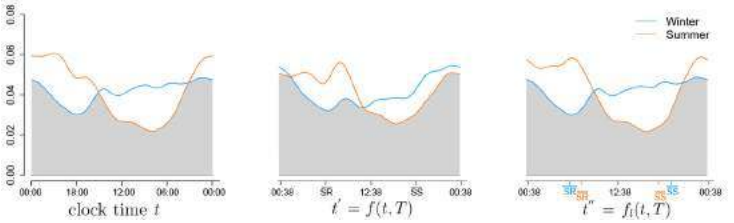

(c) Seasonal diel activity rhythms $A_{l,\bar{c}}$, $A^{'}_{l,\bar{c}}$ and $A^{''}_{l,\bar{c}}$

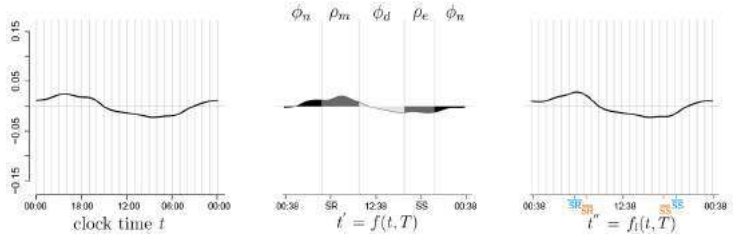

(d) Seasonal shift in diel activity rhythms $S_{,\bar{c}}$, $S^{'}_{,\bar{c}}$ and $S^{''}_{,\bar{c}}$

Figure 2.9: Seasonal shift in diel activity rhythms of the mammal community
Winter and summer diel activity rhythms of the mammal community in the Little Karoo are displayed in (a) and (c), using three different time metrics: traditional 24-hour human clock-time t and two ecological times with standardised sunrise and sunset times $t^{'}$ and $t^{''}$; the grey area being the overlap between the two probability density functions. In (a) the density functions were built using the raw camera trap data collected for the mammal community c : 4159 photo-captures in winter and 4208 photo-captures in summer. In (c) the density functions were built after attributing the same weight to every species s of the community c, independently of its photo-capture frequency.
The seasonal shifts in diel activity rhythms of the mammal community, between summer and winter, were quantified in the three different time metrics, as well as before (c) and after ($\bar{c}$) equalising every species weight to build the community diel activity rhythms (displayed in (b) and (d)). Functions $S_{,c}$, $S^{'}_{,c}$ and $S^{''}_{,c}$, as well as $S_{,\bar{c}}$, $S^{'}_{,\bar{c}}$ and $S^{''}_{,\bar{c}}$, were positive when the proportion of daily activity was higher in summer than in winter; vice versa for negative values.

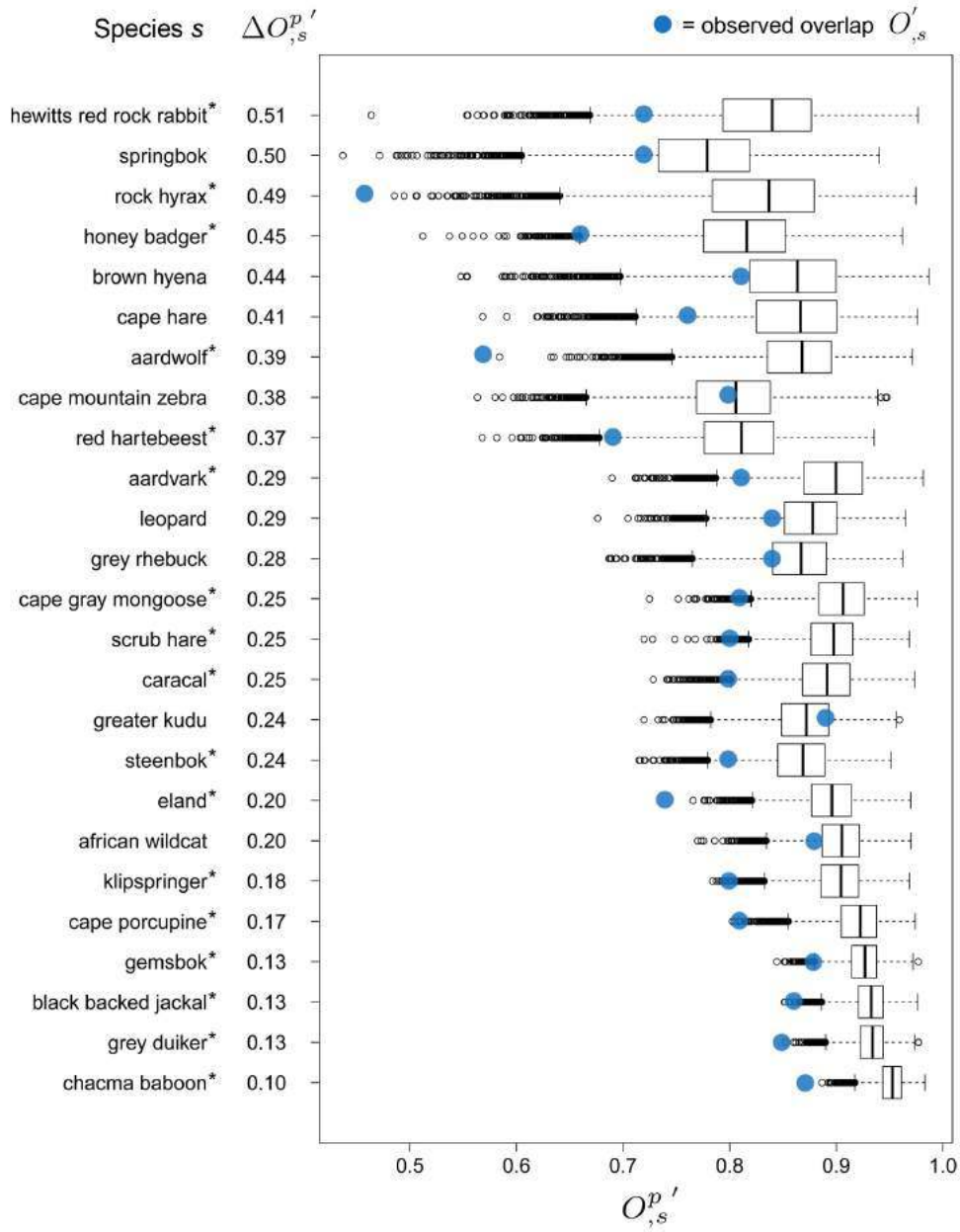

Figure 2.10: Bootstrap boxplots for each of the 25 species in the Little Karoo

Boxplots summarise the structure of the 25 $O'_{,s}$ variables, each being defined as the overlap coefficient calculated between two diel activity rhythms of species s, built with two data samples randomly selected from the original dataset collected for species s. The bootstrap analysis used $r = 10,000$ permutations p, producing 10,000 $O^{p}_{,s}{}'$ values [Chapter 2 section 2.3.3.3]. The 25 species were sorted in descending order with respect to the degree of dispersion (spread) of $O'_{,s}$, which was quantified by $\Delta O^{p}_{,s}{}'$, and which represents the versatility of the diel activity rhythm of species s, throughout a 365-day cycle. The second and third quartiles of the $O'_{,s}$ variable, are represented by the box, the median being the vertical line within the box. The blue points represent the observed value of $O'_{,s}$ calculated between the diel activity rhythms of species s in summer and in winter. * is showing next to the names of species with a significant seasonal change ($P'_{,s} < 0.05$).

Figure 2.11: Non-metric Multi-Dimensional Scaling

NMDS plot summarising the dissimilarity data between the $S'_{,s}$-curves. These curves are those of the middle column of Fig. 2.8, but are all midday centred. They illustrate the seasonal shift in diel activity rhythm of 25 mammal species s of the Little Karoo, between summer and winter.

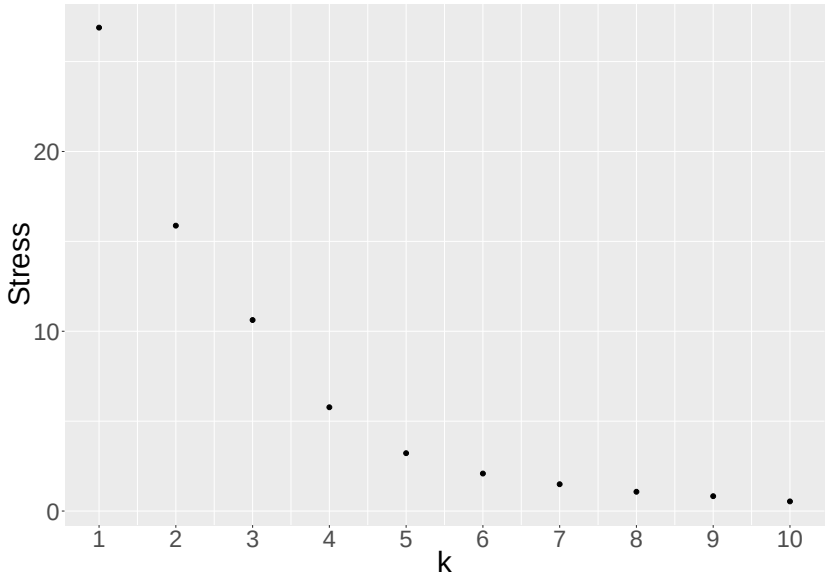

Figure 2.12: Stress values in relation to the number of dimensions k
The measure of lack of fit in NMDS is known as the 'stress' of the configuration. Non-zero stress values occur with insufficient dimensionality, and as the number of dimensions increases, the stress value will either decrease or remain stable.

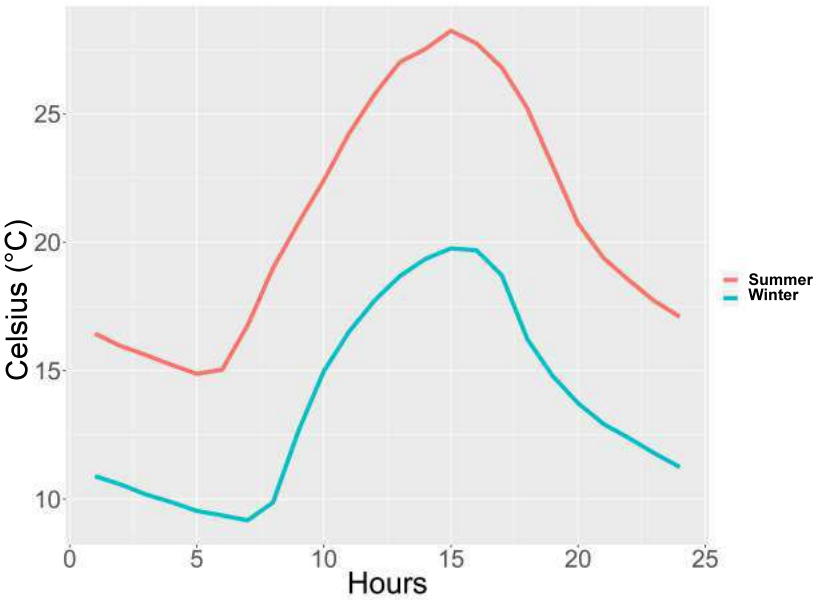

Figure 2.13: Seasonal temperatures
Hourly temperatures collected in Ladismith (Little Karoo) during winter and summer were provided by the South African Weather Service. They were averaged throughout the study period (March 2014 - August 2015).